A STUDY OF BEAM DIAGNOSTIC PROBES FOR THE TRIUMF ACCELERATOR

by

PETER WILLIAM JAMES

B.Sc., University of Victoria, 1969

A THESIS SUBMITTED IN PARTIAL FULFILLMENT OF

THE REQUIREMENTS OF THE DEGREE OF

MASTER OF SCIENCE

in the Department

of

Physics

We accept this thesis as conforming
to the required standard

[redacted]

UNIVERSITY OF VICTORIA

November 1972

ABSTRACT

Supervisor: Professor L.P. Robertson

A survey of several monitors which can be used for measuring the intensity, position, profile and energy of the proton beams to be produced at TRIUMF is presented. The survey deals in some detail with the theory of operation, design, performance and capabilities of each of the monitors discussed. Because of the large range in intensities encountered at TRIUMF, a review of both low intensity and high intensity monitors is included.

Based on the survey, we conclude that the most useful device for measuring either the intensity, position or profile of the proton beams is some type of secondary emission monitor, while the proton spectrometer proves to be the most accurate beam energy monitor. A Faraday cup incorporated as part of one of the Proton Area beam dumps is considered the best absolute monitor for calibrating other intensity monitors.

ACKNOWLEDGEMENTS

The author wishes to thank Professor L.P. Robertson for his guidance during the progress of this work.

For reading the manuscript and offering many valuable comments, the author is indebted to Dr. R.M. Pearce, Dr. D.E. Lobb, Dr. H. Dosso, and Dr. R.N. O'Brien. The author also wishes to thank his wife, Elizabeth, for the careful typing of the final manuscript.

Financial support in the form of a postgraduate scholarship from the National Research Council of Canada is gratefully acknowledged.

TABLE OF CONTENTS

LIST OF TABLES

LIST OF FIGURES

CHAPTER 1

INTRODUCTION

It is important for the successful operation of a particle accelerator facility to be able to measure easily and accurately such properties of the external beams extracted from the accelerator as the energy, energy spread, intensity, and intensity distribution. Especially during the commissioning period, accurate measurements of the beam parameters are required in order to optimize the performance of the accelerator and to properly adjust the settings of the beam transport magnets so as to obtain efficient transmission of the beams to targets in the experimental areas. The purpose of this work is to review the various types of monitors which may be used to measure the beam parameters. The study can be used as a basis for deciding which devices are suitable for monitoring the external proton beams to be produced at TRIUMF.

A brief description of the TRIUMF facility and a summary of the characteristics of the proton beams are presented in Chapter 2. The high energy and intensity of the beams present some unique problems in the choice of suitable monitors. Many devices used for monitoring low energy beams are not suitable for use at TRIUMF because they rely on stopping all of or a fraction of the beam. Several types of monitors, such as geiger tubes and spark chambers, which rely on the detection of individual particles cannot be used because of the large intensities of the proton beams. The large

range in intensities which will be used also makes it difficult to find a monitor capable of operating over the full range. The time structure of the beams restricts the use of such devices as induction toroids, capacitive pickups, and microwave cavities commonly used at many high energy facilities.

In order to specify the monitors required at TRIUMF, a monitoring system for the first section of one of the proton beam lines is suggested and discussed in Chapter 3. Following this a summary is made of several monitors reported in the literature and presently in use at various accelerators, and an analysis is made of those suitable for TRIUMF. Extensive use has been made of the excellent reviews published in the proceedings of conferences held at Daresbury (Hatton and Lowndes 1968), LAMPF (Macek et al. 1971), Chicago (Shea 1965; 1971), and Washington (Shea 1967; 1969). Additional information was taken from books edited by Ritson (1961), Yuan and Wu (1961), Neal (1968), and La Postolle and Septier (1970), as well as from the numerous papers listed in the bibliography.

CHAPTER 2

CHARACTERISTICS OF THE TRIUMF PROTON BEAMS

2.1 The TRIUMF Facility

The TRIUMF cyclotron presently under construction at the University of British Columbia is a six-sector, azimuthally varying field (A.V.F.), isochronous machine designed to accelerate negative hydrogen ions to a maximum energy of 525 MeV. The acceleration of H^- ions enables high energy proton beams to be extracted with essentially 100% efficiency. The protons are produced by passing the ions through a thin foil (e.g. 4 mg/cm^2 carbon) which causes the two electrons to be stripped from each ion. By changing the radial position of this foil, the energy of the extracted proton beam can be varied continuously from 150 to 525 MeV. At the outset, the energy resolution of the beam is expected to be ± 600 keV, while the R.F. phase acceptance will be 40° or 11%; giving a microscopic duty cycle of beam on for 5 nsec every 43 nsec, as the accelerating R.F. field has a fundamental frequency of 23.1 MHz. As soon as possible, a third harmonic component will be added to the R.F. field thereby improving the microscopic duty cycle to 23%, i.e. beam on 10 nsec every 43 nsec. Because it is a fixed frequency cyclotron, the macroscopic duty factor is 100%, i.e. the R.F. accelerating voltage is on continuously.

A general plan of the TRIUMF facility is shown in Fig. 2.1. Although the six-fold symmetry of the cyclotron magnet will permit

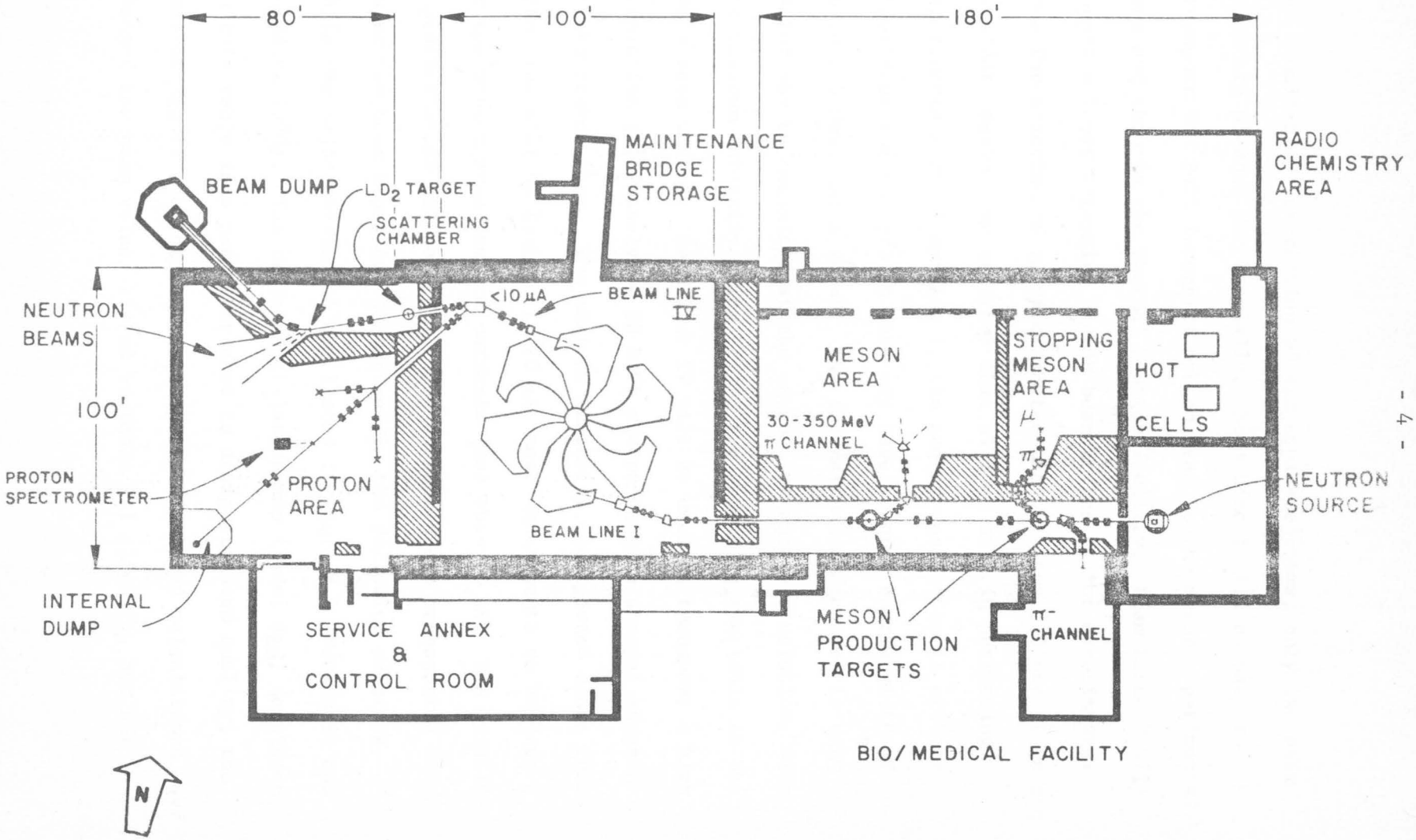

Fig. 2.1 Layout of beam lines and experimental areas at TRIUMF (May 1972)

the simultaneous extraction of six separate beams, only two beam lines are planned for initially. Beam Line I will be used to transport the full intensity proton beam to the meson experimental area and then to the thermal neutron facility. Beam Line IV will supply a lower intensity proton beam to the proton experimental area for experiments using extracted proton beams. Since it is the secondary mesons and neutrons that will be used in performing experiments along Beam Line I, the energy resolution is of less importance and the proton beam may have a total energy width of up to 2.5 MeV. As a result, the intensity and microscopic duty factor may be maximized at the expense of energy resolution, with the maximum intensity being set by the shielding available in the meson beam tunnel. Beam Line IV will be used to transport a high resolution (ultimately, ± 50 keV) proton beam to several targets in the proton area. The maximum intensity transported along this beam line will be limited to 10 μA; most experiments to be done in the proton area require currents less than 1 μA. The detailed characteristics of the beams to be extracted and transported down these two beam lines are summarized in the following sections, while the major parameters are listed in Table 2.1 (Mackenzie and Craddock 1970). The radial oscillation amplitude, A_{Rm}, mentioned in this table is a parameter used to designate beam quality; the smaller A_{Rm} is the better beam quality. Improved calculations have changed the beam values listed in Table 2.1 slightly, but not

T A B L E 2.1

Energy Spread and Beam Quality on Leaving the Stripping Foil (foil scattering not included)

Mode of operation	Normal operation - wide stripper														
Radial oscillation amplitude at 30 MeV (in.)	0.40					0.25					0.14				
Fraction of 3rd harmonic (%)	0/-14					0/-14					0/-14				
Phase spread (°)	40/83					30/76					15/65				
Microscopic duty factor (%)	11/23					8/21					4/18				
Pulse length (nsec)	4.8/10					3.6/9.2					1.8/7.8				
α Maximum current obtainable (μA)	440/920					320/840					160/720				
β Maximum current permissible (μA)	850	650	250	175	100	675	500	250	175	100	500	400	250	175	100
Energy (MeV)	150	200	300	400	500	150	200	300	400	500	150	200	300	400	500
* Total ΔE (MeV)	1.6	1.7	1.8	1.9	2.3	1.2	1.4	1.4	1.4	1.6	0.8	1.0	1.1	1.1	1.2
* Horizontal spot size (in.)	0.57	0.56	0.33	0.20	0.13	0.43	0.42	0.33	0.20	0.13	0.34	0.31	0.30	0.20	0.13
* Horizontal divergence (mr)	3.4	2.7	2.1	1.7	2.6	2.5	2.0	1.6	1.6	1.7	1.4	1.2	1.1	1.0	0.9
* Vertical spot size (in.)	0.46	0.45	0.44	0.42	0.40	0.46	0.45	0.44	0.42	0.40	0.46	0.45	0.44	0.42	0.40
* Vertical divergence (mr)	0.80	0.68	0.58	0.51	0.45	0.80	0.68	0.58	0.51	0.45	0.80	0.68	0.58	0.51	0.45

The current available will be the lower of "α" and "β". α is the maximum current obtainable based on a 2 mA ion source, a factor 2 bunching, and duty factor and slit restrictions. β is the maximum current permitted by power dissipation in the stripping foil (for a foil lifetime > 1 week) and/or space charge effects. * The energy, spot size and divergence spreads are all "total widths" and include tails.

sufficiently to alter conclusions about monitor requirements.

2.2 Beam Intensity

During the first three months of operation, the internal beam dynamics of the cyclotron will be thoroughly investigated. The average beam intensity will be kept at or below 200 nA, with most of the beam being lost inside the machine. In order to overcome this restriction in beam current, the use of a chopped beam simulating full current conditions has been proposed (Duelli 1969; 1971). Under this scheme, the macroscopic duty cycle of the accelerator will be limited to values less than 1.5% with beam pulse widths of 50 nsec or more. The frequency of these pulses is determined by the duty cycle required, but would always be less than 230 kHz. The advantage of this technique is that the beam dynamics of the accelerator can be studied under high intensity conditions without the problem of excessive activation caused by a high intensity proton beam.

Beam dynamics studies will continue during the next three months, but the emphasis will shift to the external beam lines. The alignment of the various quadrupoles and bending magnets will be checked, using the actual beam as the probe. In addition, the beam emittance and energy definition will be investigated. The chopped beam can be used to great advantage during this period. The average intensity of the extracted beams will be held below

100 nA for beam diagnostic purposes, but will increase slowly to 1 μA as preliminary nuclear physics experiments get under way. Within the following six months, the external beam intensity will be raised to a total intensity of 10 μA.

At the beginning of the second year the cyclotron will be operated at full intensity. The maximum intensities available during full beam operation are set by the requirement that the total beam spill inside the cyclotron be less that 20 μA at 500 MeV or an equivalent power loss of 10 kW. This criteria will prevent excessive activation of the cyclotron, and will enable servicing to begin within a reasonable period after shutdown. The beam spill is caused both by the electric dissociation of the H^- ions as they travel through the cyclotron's magnetic field and by the stripping of the ions through collisions with the residual gas molecules in the vacuum tank. On the basis of the expected electric stripping losses shown in Table 2.2 (Auld 1971) and the 4% gas stripping loss expected for a pressure of 4×10^{-8} Torr, the values for the maximum intensities permitted along Beam Line I assuming a 10 kW beam spill within the cyclotron have been calculated and are given in Table 2.2. Although it is expected that these intensities can be obtained from the 2 mA ion source being developed provided the third harmonic is used in the R.F. accelerating voltage, the limitations which arise because of power dissipation in the stripping foil (Mackenzie, 1969) have not been taken into consideration. As a result of the strong

T A B L E 2.2

Beam Intensity Limits Set by Activation of the Accelerator

Beam Energy (MeV)	Electric Stripping Loss (%)	Maximum Intensity (μA)
525	22.5	70
500	13.5	115
450	3.0	320
400	0.5	560
300	0	750
200	0	1250

magnetic fields surrounding this foil, the two electrons which are stripped from each H^- ion will spiral around and deposit their total energy in the foil (250 keV/electron for 500 MeV ions). The foil must therefore be thick enough to have a reasonable lifetime allowing for the evaporation of material from its surfaces. On the other hand, if it is too thick the multiple coulomb scattering introduced will seriously degrade the quality of the extracted beams such that the acceptance of the transport systems will be exceeded. Mackenzie and Craddock (1970) have calculated the maximum intensities that can be extracted using a 4 mg/cm^2 carbon foil assuming a lifetime of one week or more. Their results are shown in Table 2.1, and for energies below 500 MeV they indicate a significant reduction from the figures quoted above.

2.3 Energy Resolution

The energy resolution of the extracted beams is determined primarily by the amplitude of the radial oscillations at the extraction radius, by the energy gain per turn in the accelerator, and by the spread in the phase of the H^- ions with respect to the peak in the R.F. voltage. Calculations show (Richardson 1969) that the resolution of the 500 MeV beam using a wide stripping foil, i.e. with a width greater than two turn separations so that the entire beam is intercepted, is $\pm$ 600 keV. As seen from Table 2.1, the resolution is improved at lower energies. Low energy defining slits placed at

a radius of 70" in the accelerator can reduce the energy spread to ± 100 keV at 500 MeV at the expense of a smaller microscopic duty factor and a lower intensity of 2 μA maximum.

Various other methods have been suggested (Richardson 1969; Richardson and Craddock 1969) for improving the energy resolution of the proton beams and are summarized in Table 2.3.

2.4 Beam Emittance, Divergence and Lateral Dimensions

The lateral dimensions and angular divergence of the beam given in Table 2.4 represent the semi-axes of the phase space distribution at the exit of a 4 mg/cm^2 carbon stripping foil. θ_o and ϕ_o, the angular divergence in the horizontal and vertical directions, respectively, were calculated by adding the half-divergence values for the beam incident on the foil, as given in Table 2.1, in quadrature with twice the rms projected scattering angle, σ_{RG}, for such a foil. σ_{RG} was calculated from the following equation (Rossi and Greisen 1941)

$$\sigma_{RG} = \frac{21.2}{pv} \sqrt{\frac{t}{2L_{rad}}} \qquad (2.4.1)$$

where t is the foil thickness in gm/cm^2, L_{rad} is the radiation length of the foil material in gm/cm^2, and p and v are the average

T A B L E 2.3

Summary of the Main Characteristics of the 500 MeV High Resolution Proton Beams

Mode of Operation	Full Width Energy Spread (keV)	Phase Acceptance (°)		Estimated Intensity (μA)	Microscopic Duty Factor (%)
Raw beam	± 600	± 30		100	15
		± 50	(3rd)	100	27
Low energy slits 0.032 in.	± 100	± 1.8		2	1
		± 14	(3rd)	16	8
Separated turn acceleration	± 50	± 0.5		5	0.3
	± 25	± 6.7	(3rd)	30	3.7
Final orbit selection	± 60	± 0.5		0.05	0.3
		± 5.0	(3rd)	0.5	2.8

(3rd) indicates that the proper mixture of third harmonic of the RF voltage is used.

T A B L E 2.4

Lateral Dimensions and Angular Divergence of the Beam on Leaving a 4 mg/cm^2 Carbon Stripping Foil

Radial oscillation amplitude at 30 MeV (in)	0.40					0.25					0.14				
Energy (MeV)	150	200	300	400	500	150	200	300	400	500	150	200	300	400	500
Horizontal spot size x_o (mm)	7.24	7.11	4.19	2.54	1.65	5.46	5.33	4.19	2.54	1.65	4.32	3.94	3.81	2.54	1.65
Horizontal divergence θ_o (mrad)	2.00	1.57	1.19	0.95	1.35	1.63	1.28	0.97	0.91	0.92	1.26	1.00	0.78	0.66	0.57
Vertical spot size y_o (mm)	5.84	5.72	5.59	5.33	5.08	5.84	5.72	5.59	5.33	5.08	5.84	5.72	5.59	5.33	5.08
Vertical divergence ϕ_o (mrad)	1.12	0.87	0.62	0.50	0.42	1.12	0.87	0.62	0.50	0.42	1.12	0.87	0.62	0.50	0.42

momentum and velocity of the beam on passing through the foil. According to the theory derived by Rossi and Greisen, $2\sigma_{RG}$ should include 95.5% of the coulomb multiply scattered beam. However, as shown by James (1971), a more accurate theory developed by Molière (1948) predicts that in the case of 500 MeV protons incident on a 4 mg/cm^2 foil 98.3% of the scattered beam will lie within $2\sigma_{RG}$.

Although the foil increases the beam divergence significantly, increases in the lateral dimensions of the beam are negligible since the rms displacement, l_{rms} due to multiple coulomb scattering is given by

$$l_{rms} = t\sigma_{RG}/\sqrt{3} \qquad (2.4.2)$$

and is always less than 10^{-2} mm for a 4 mg/cm^2 carbon foil. Therefore, the horizontal and vertical dimensions of the beam, x_o and y_o, shown in Table 2.4 are taken directly from the results of Mackenzie and Craddock (1970) listed in Table 2.1.

For the purpose of calculating the lateral extent of the beam at various locations along the beam lines, it is convenient to approximate the beam density distribution in the phase space having co-ordinates of lateral displacement, x and y, and divergence, θ and ϕ, for the horizontal and vertical directions respectively as being contained in an elliptical area. The areas

of these ellipses are defined as the x and y emittances, ϵ_x and ϵ_y. The emittance at the stripping foil has been assumed to be given by

$$\epsilon_x = x_o \theta_o \text{ (mm-mrad)} \tag{2.4.3}$$

$$\epsilon_y = y_o \phi_o \text{ (mm-mrad)} \tag{2.4.4}$$

Since the x, y, and z motions of the beam are independent, according to Lioville's theorem (Banford 1966, p. 10) ϵ_x and ϵ_y will remain constant at all points along any beam line composed of quadrupoles and bending magnets provided no material is placed in the beam. Assuming this to be the case the beam envelopes, which give the variation in the horizontal and vertical beam widths along the beam line, have been calculated for the first section of Beam Line I at 200 and 500 MeV and are shown in Figs. 2.2 and 2.3. These envelopes were calculated using the program TRANS (Chan et al. 1972), the beam parameters listed in Table 2.4, and the beam transport systems designed by Lobb (1971).

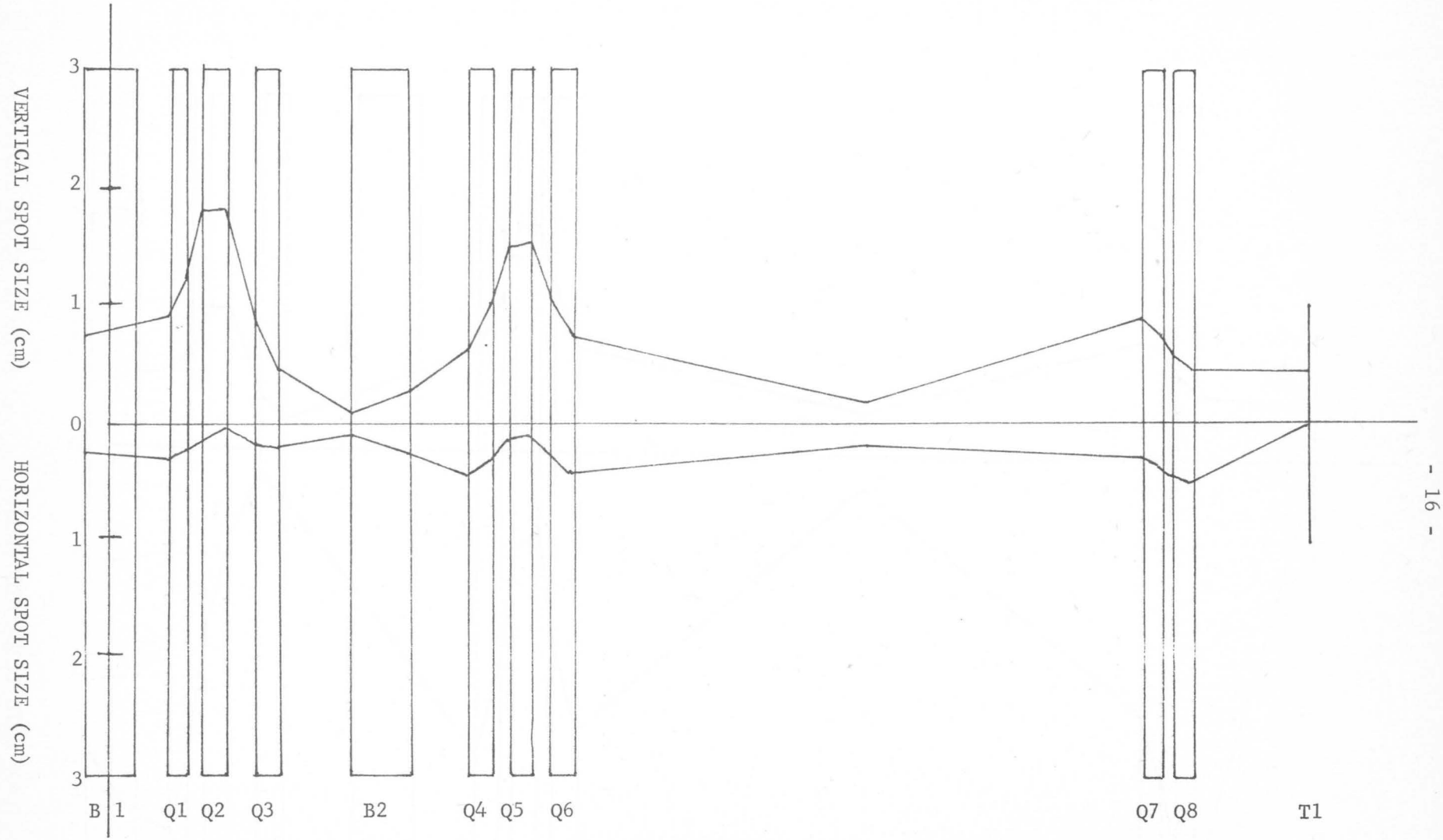

Fig. 2.2 Horizontal and vertical beam envelopes along the first section of Beam Line I for a 500 MeV beam (A_{Rm} = 0.14")

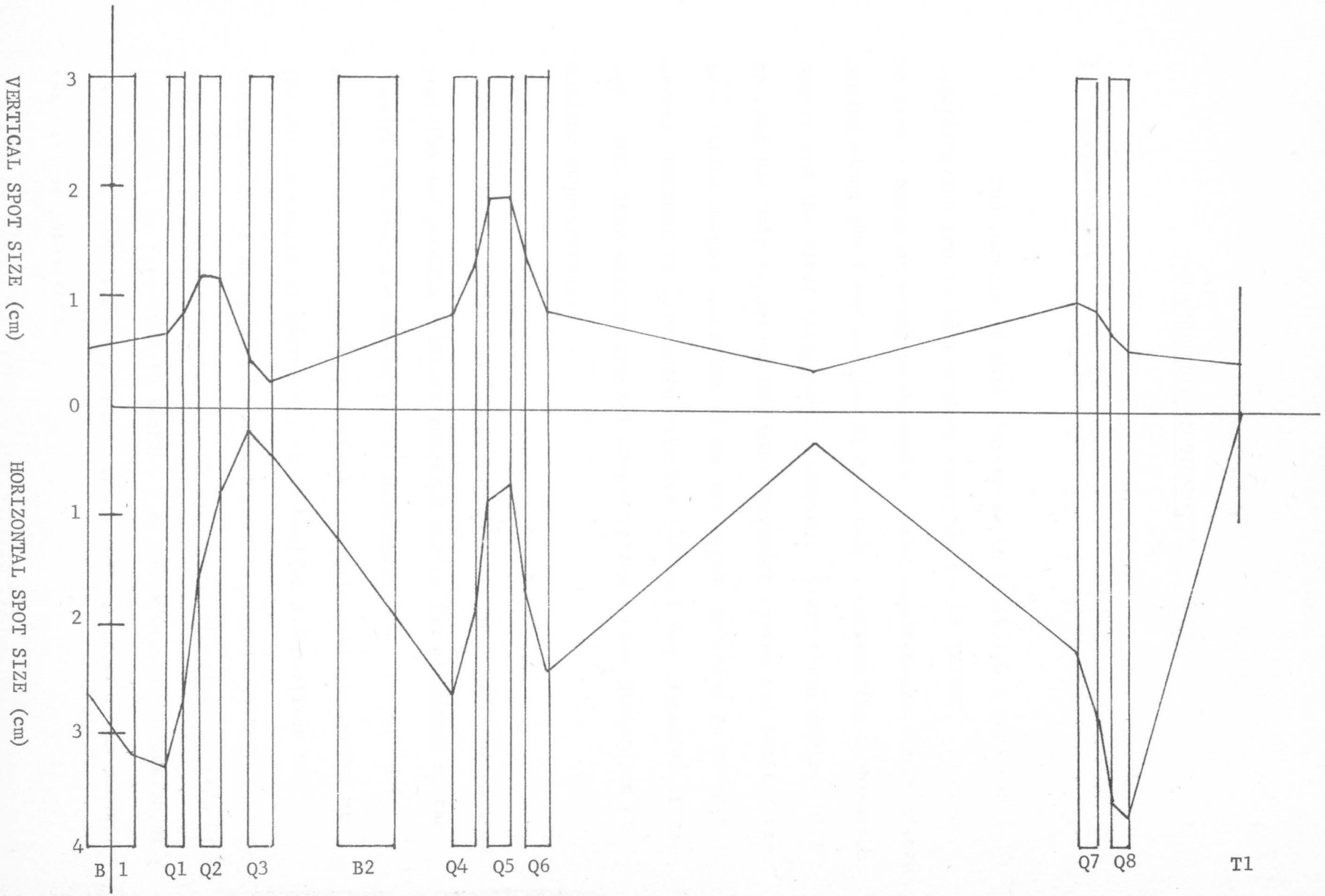

Fig. 2.3 Horizontal and vertical beam envelopes along the first section of Beam Line I for a 200 MeV beam (A_{Rm} = 0.40")

CHAPTER 3

BEAM MONITOR REQUIREMENTS AT TRIUMF

3.1 Introduction

The purpose of this chapter is to establish a philosophy regarding the proton beam monitor requirements at TRIUMF. In order to have a basis on which to determine these requirements, the monitors needed along the first section of Beam Line I between the combination magnet and the first target are discussed. Since these devices will be used not only to set up the beam transport system and monitor the beam during normal operation of the cyclotron but also to measure several parameters associated with the internal beam dynamics of the cyclotron, they deserve special consideration in any discussion of monitor requirements.

Sections 3.2 and 3.3 of this chapter deal with the various position and profile monitors required during the alignment of the transport system and during normal beam operation. Section 3.4 considers the problem of the various intensity monitors needed at the divers stages of operation, while Section 3.5 outlines the requirements of the profile monitors used to measure beam emittance. A summary of all the monitors to be used along the first section of Beam Line I is presented in Section 3.6, along with a discussion of some of the more general problems which must be overcome in measuring the various parameters.

3.2 Transport System Setup and Alignment

The ten beam monitor locations suggested for the alignment of the first section of Beam Line I are shown in Fig. 3.1. The devices used at these locations must be able to monitor beams of very low currents ($\sim$ 1 nA) and current densities ($\sim$ 1 nA/cm^2), since the intensities used during beam alignment are very small.

The monitors located at the various positions shown in Fig. 3.1 will be used for several purposes. In particular, those devices located at points 1,2, and 3 are required in order to determine the position and direction of the beam in both the horizontal and vertical planes as it leaves the combination magnet, B1. This information will enable the current setting of this magnet and the azimuthal position of the stripping foil to be adjusted so as to correctly extract the proton beam from the cyclotron. The radial position of this foil is of course determined by the desired beam energy. Measurements of the horizontal beam position at points 4 and 5 will be used to establish the correct current setting for the 20° bending magnet, B2. Position monitors located at points 6,7, and 9 will be used to guide the beam to the experimental target T1.

Estimates of the accuracies, $\delta\theta$ and $\delta\phi$, to which the horizontal and vertical beam directions can be determined using the

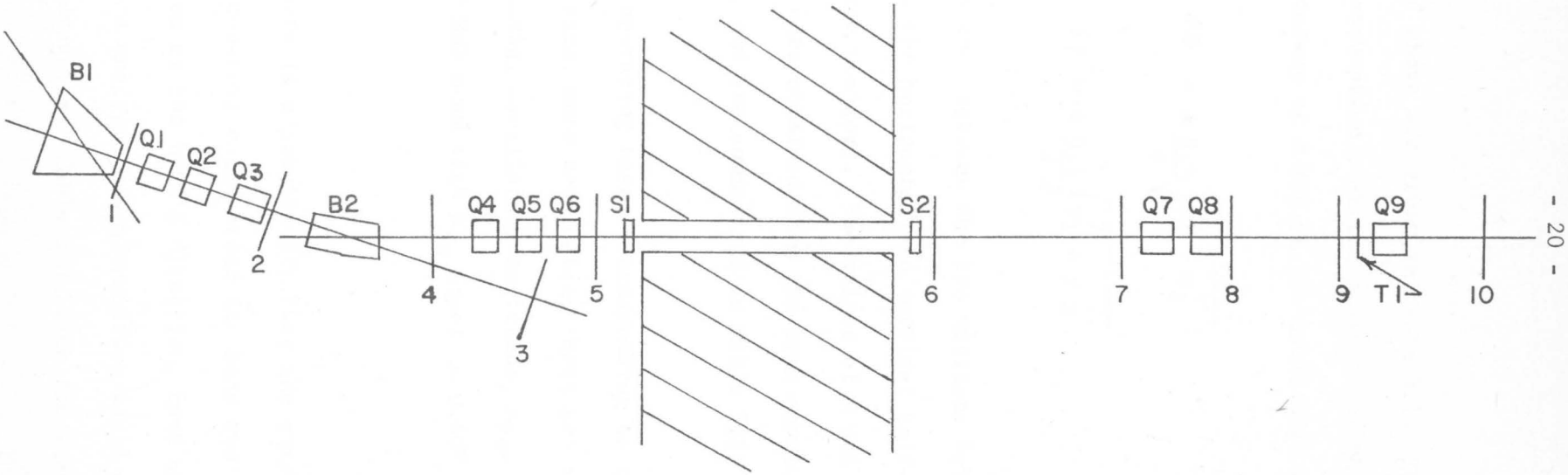

Fig. 3.1 Beam monitor locations for the first section of Beam Line 1

monitors discussed above are given in Table 3.1. These calculations are based on the assumption that the position of the beam can be measured to an accuracy of ± 20% of the total beam width. Under this condition,

$$\delta\theta = \pm \frac{0.4}{d} \sqrt{x_1^2 + x_2^2} \qquad (3.2.1)$$

$$\delta\phi = \pm \frac{0.4}{d} \sqrt{y_1^2 + y_2^2} \qquad (3.2.2)$$

where d is the distance between the two monitors being used, and x_1, x_2, y_1, and y_2 are the horizontal and vertical half-widths of the beam as measured by these monitors. The values of x and y at the various monitor locations were obtained from the beam envelopes shown in Figs. 2.2 and 2.3, and are summarized in Table 3.2.

The two operating cases corresponding to the smallest and largest beam spot sizes were considered; these are the 500 MeV beam with an internal radial oscillation amplitude, A_{Rm}, of 0.14" at 30 MeV and the 200 MeV beam with A_{Rm} equal to 0.40" at 30 MeV, respectively.

Since there is a possibility that the quadrupoles located between a pair of monitors could steer the beam and thus cause errors in the determination of the beam's direction, care must be exercised if these magnets are excited. An alternative would of course be to turn off these quadrupoles. Table 3.3 lists the angular resolutions

T A B L E 3.1

Accuracies to Which the Horizontal and Vertical Directions of the Beam can be Determined Using the Monitors Indicated

Monitors Used	Distance, d Between the Monitors (m)	$\pm\delta\theta$ (mrad)		$\pm\delta\phi$ (mrad)	
		200 MeV	500 MeV	200 MeV	500 MeV
1 and 2	3.0	4.3	0.45	0.94	1.4
1 and 3	9.0	2.2	0.35	0.68	0.64
4 and 5	3.5	3.7	0.62	1.4	0.96
6 and 7	5.0	1.9	0.29	0.84	0.66
6 and 9	9.0	0.14	0.10	0.26	0.22

T A B L E 3.2

Lateral Dimensions of the Beam at the Various Monitor Locations

Location	x (mm)		y (mm)	
	200 MeV	500 MeV	200 MeV	500 MeV
1	32	2.7	6.5	9.0
2	4.2	1.8	2.6	4.5
3	37	7.2	14	11
4	22	3.4	7.9	4.3
5	24	4.2	8.9	7.2
6	3.0	2.0	3.5	1.8
7	23	3.0	9.9	8.1
8	30	3.8	5.1	4.6
9	0.74	0.5	4.4	4.4
10	30	3.8	4.9	4.5

T A B L E 3.3

Accuracies to Which the Horizontal and Vertical Directions of the Beam can be Determined When the Quadrupoles are Off

Monitors Used	Distance d(m)	Quadrupoles Not Excited	$\pm\delta\theta$ (mrad)		$\pm\delta\phi$ (mrad)	
			200 MeV	500 MeV	200 MeV	500 MeV
1 and 2	3.0	Q1,Q2, & Q3	6.5	0.60	1.5	2.0
1 and 3	9.0	Q1,Q2, & Q3	2.6	0.30	0.78	0.90
4 and 5	3.5	Q4,Q5, & Q6	5.0	0.94	1.7	1.4
6 and 7	5.0	------	1.9	0.29	0.84	0.66
6 and 9	9.0	Q7 & Q8	1.6	0.22	0.68	0.56

T A B L E 3.4

Lateral Dimensions of the Beam When the Quadrupoles Listed are Off

Location	Quadrupoles Not Excited	x(mm)		y(mm)	
		200 MeV	500 MeV	200 MeV	500 MeV
1	------	32	2.7	6.5	9.0
2	Q1,Q2, &Q3	37	3.6	9.3	12
3	Q1,Q2, & Q3	48	6.4	16	18
4	------	22	3.4	7.9	4.3
5	Q4,Q5, &Q6	38	7.5	12	11
6	------	30	2.0	3.5	1.8
7	------	23	3.0	9.9	8.1
8	Q7 & Q8	29	3.6	12	10
9	Q7 & Q8	37	4.4	15	13
10	Q7,Q8 & Q9	44	5.4	18	15

expected if this were done. The angular resolutions obtainable are larger when the quadrupoles are off; however there is less chance of error in the actual measurement of the beam direction. It is therefore recommended that the initial measurements be made with the quadrupoles off. The quadrupoles could then be turned on and more accurate measurements made.

Given the spot sizes indicated in preceeding tables and the criteria that the position of the beam be known to ± 20% of the total beam width, the monitors used at the above locations should all have a position resolution of 1 to 2 mm except in the case of monitor 9 where a resolution of a few tenths of a millimeter is required.

As well as being used to measure beam position, several of the monitors already discussed are required to measure the profile of the beam. These include the devices at points 2 and 5 which will be used primarily to check that the transport system is operating correctly. With the transport system in its normal operating mode, the monitor at 2 can also be used for a crude energy spread measurement as the dispersion of the beam is quite large at the exit of quadrupole Q3. Such a measurement cannot be performed downstream of the 20° bending magnet since, under normal operating conditions, the transport system is achromatic from that point onwards. Further measurements of the profile of the beam are required at points 8,9, and 10 in

order to determine the beam size at the target and to insure that there is a waist in the horizontal plane located within 10 to 20 cm of T1. Profile measurements at the latter three locations can also be used to determine the emittance of the beam in each plane, although a more accurate determination of the beam emittance can be made by measuring the size of the beam at points 5 and 7. A discussion of the methods used to measure the beam emittance is given in Section 3.5.

The monitors used to measure beam profiles must be able to detect changes in these profiles which occur over 20% of the total beam width. They therefore should have the same resolutions as the position monitors discussed above. Note that a single profile monitor can be used at those locations where position and profile measurements are required, that is at points 2,5,7, and 9.

3.3 Normal Beam Operation

When Beam Line I is run under normal operating conditions the number of monitor locations can be reduced to four; one each at points 2,5,8, and 9. The devices at these points should be designed to continuously monitor the beam at intensities ranging from 1 nA to 0.5 mA. Because of this large range in intensities, two sets of monitors may have to be constructed, one each for low ($< 1.0\ \mu A$) and for high intensity operation. If this is necessary, the low intensity monitors should be designed so that they can also

be used during beam alignment.

At each of the locations mentioned above, the position, size and intensity of the beam should be measured. However, since only an indication of the size of the beam and not a detailed measurement of its profile is required, a profile resolution equal to 50% of the minimum total beam widths expected at the monitor locations is certainly adequate. With the exception of the monitor at point 9, this figure corresponds to an absolute resolution of 3 to 5 mm. This high a resolution will also permit the position of the beam to be measured with sufficient accuracy.

The higher resolution required at location 9 is a direct result of the small beam size at T1 (typically 1.0 mm x 1.0 cm) as well as the small size of the target itself (0.5 cm x 1.5 cm). Because of their relative sizes, the beam must be positioned to within 0.5 mm of the target's centre in order to insure that all the beam hits the target. This sets the position resolution in each plane to 0.5 mm. The higher resolution in profile is required to insure that the beam does not get too small at T1. If this were to happen during periods when large intensities were being used, the resulting current densities could cause damage to the target and its support structure. These densities should be kept below 3 mA/cm^2 (Hodges 1971). In order to accomplish this, a reduction in the size of the beam of 50% of its optimum width should be detectable.

This sets the profile resolution to 0.5 mm in the horizontal plane and 0.5 cm in the vertical plane. The horizontal resolution demanded here will also permit the horizontal beam-width to be measured accurately enough so that the performance of the pion channel located immediately downstream of T1 can be optimized (Reeve 1971). A profile monitor at location 7 can also be used to insure that the beam does not get too small at T1 since a small beam at T1 arises only if the beam is small at the entrance of quadrupole Q7.

3.4 Intensity Monitor Requirements

The intensity monitors required along the first section of Beam Line I can be divided into two groups. The first group will be used during beam alignment and the initial stages of normal beam operation. It includes monitors at locations 1,2,3,4,5, and 9 which must all be capable of measuring average currents as small as 1 nA. The absolute accuracy required is of the order of 10 to 20%. The second group which includes devices at points 2,5, and 9 will be used during high intensity operation. These monitors should be able to detect currents of the order of a few microamps and larger. An absolute accuracy of the order of 5% should be adequate for most purposes. All of the devices discussed in this section should, if possible, have a linear response over the full range in intensities for which they are to be used. The intensity limits discussed above are based on the beam intensities expected during the various stages of cyclotron operation as outlined in Section 2.2.

Most of the intensity monitors used will be relative rather than absolute in nature and will require periodic calibration against some absolute standard. It is suggested that a Faraday cup located at point 3 or at the beam dump in the proton area be used as such a standard.

Although most of the devices will be designed to measure average intensities, it may be advantageous to construct some which are sensitive to peak currents. This would be especially advantageous during beam alignment as it has been suggested that one operate during this period with a much reduced microscopic duty factor (see Section 2.2). The peak currents would be at least 100 times larger than the average currents and should therefore be easier to measure.

3.5 Beam Emittance Measurements

Two methods which can be used to measure the emittance of the beam by measuring beam widths are discussed in this section (Banford 1966). Both of these methods assume the beam to have elliptical phase space contours.

The first makes use of the equation for the variation in beam envelope size, x, as the beam travels through a drift space.

This equation is given by (Banford 1966, p.24)

$$x^2(z) = x_o^2 + z^2 x_o'^2 \qquad (mm^2) \qquad (3.5.1)$$

where z is the distance along the beam direction as measured from a waist, and x_o and x_o' are the half-width and divergence of the beam ellipse in the horizontal plane at that waist. Using this equation and the results from the measurement of x at three points in the drift space, the horizontal emittance ϵ_x can be determined from the following equations

$$x_o'^2 = \frac{x_1^2 + x_3^2 - 2x_2^2}{2a^2} \qquad (mrad^2) \qquad (3.5.2)$$

$$b = \frac{x_1^2 - x_3^2}{4ax_o'^2} \qquad (m) \qquad (3.5.3)$$

$$x_o^2 = x_2^2 - b^2 x_o'^2 \qquad (mm^2) \qquad (3.5.4)$$

$$\epsilon_x = x_o x_o' \qquad (mm\text{-}mrad) \qquad (3.5.5)$$

where a is the separation in metres between the monitors and b is the distance in metres from the centre monitor to the waist as shown in Fig. 3.2. A similar set of equations exists for y, y_o' and ϵ_y. The locations of the waists in the x and y planes will not in general coincide.

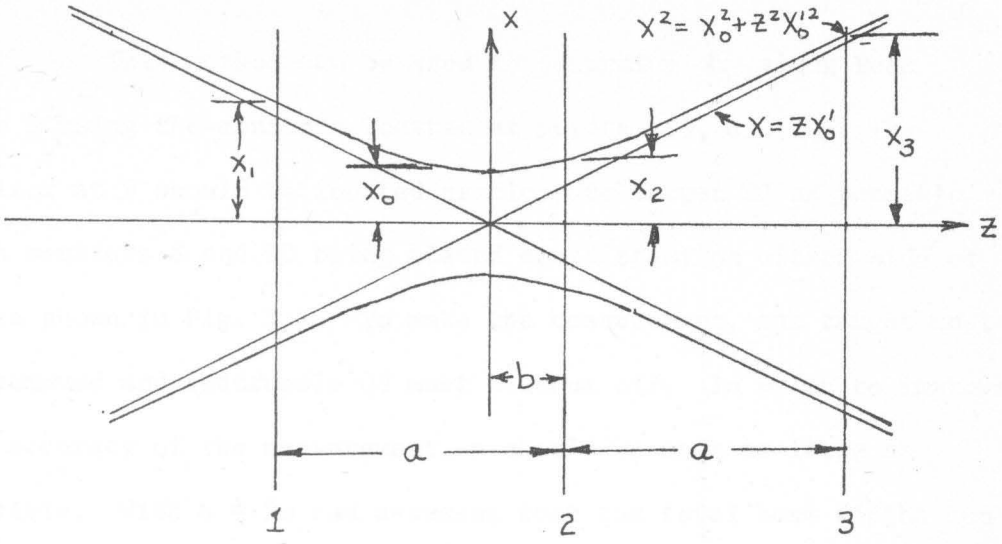

Fig. 3.2 The measurement of beam emittance using three profile monitors in a drift space

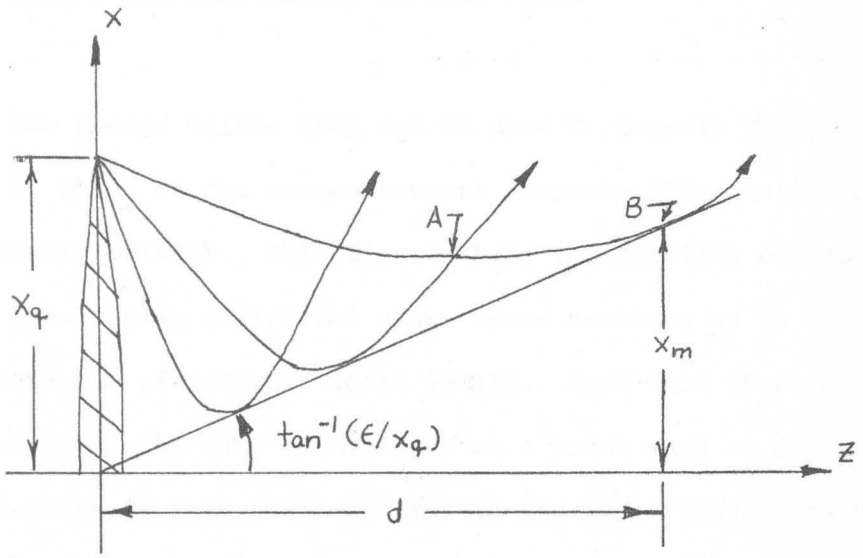

Fig. 3.3 The measurement of beam emittance using the common tangent technique

This method can be used to determine ϵ_x along Beam Line I using the monitors located at points 8,9, and 10. The monitor at 9 should be located as close to target T1 as possible, with monitors 8 and 10 being placed equidistant on either side of T1 as shown in Fig. 3.1. To make the measurement, the target must be removed and quadrupole Q9 must be shut off. In order to improve the accuracy of the measurement, a should be made as large as possible. With a = 2m and assuming that the total beam widths can be measured to ± 20%, ϵ_x can be determined to an accuracy of about ± 30% in all cases. The small divergence of the beam in the y plane at T1 prevents ϵ_y from being measured to better than a factor of 2 or 3 using this method. The position of the waist in the horizontal plane can be measured to an accuracy of ± ¼ m using equation 3.5.3, again assuming a 20% uncertainty in spot size.

The second method that can be used to measure the beam emittance is based on the common tangent property illustrated in Fig. 3.3 (Banford 1966). This figure shows the profiles of a constant emittance beam having elliptical phase space contours as it emerges from a quadrupole of variable focal length. Note that there are two profiles yielding the same beam radius at a point such as A. However, at point B there is only one such profile and it is tangent to a line of slope ϵ/x_q where ϵ is the beam emittance and x_q is the semi-width of the beam at the quadrupole. The method used to determine ϵ is to measure the beam width as a function of magnet strength at some convenient distance d metres downstream of the magnet and to note

the minimum semi-width x_m (mm). The emittance is then given by

$$\epsilon_x = x_m x_q / d \qquad \text{(mm-mrad)} \qquad (3.5.6)$$

Similarly

$$\epsilon_y = y_m y_q / d \qquad \text{(mm-mrad)} \qquad (3.5.7)$$

In order that x_m and y_m are large enough to obtain accurate measurements, d should be as large as possible. This method can be used by observing the profile at location 7 as the strength of quadrupole Q6 is varied. x_q and y_q are measured using monitor 5. Assuming the beam widths at 5 and 7 can be measured to $\pm$ 20%, both ϵ_x and ϵ_y can be measured to $\pm$ 28%. The monitors at 5 and 7 must have a resolution of 1 to 2 mm to accomplish this as the minimum total beam widths in either plane at these locations is of the order of 5 mm.

The second method is limited to those periods when the beam is run at low intensities, unless beam spill can be accomodated.

3.6 Additional Limitations on Monitor Design

Several problems must be overcome in order that monitors can be placed at the locations shown in Fig. 3.1. One of these involves the beam degradation introduced by those monitors which require small amounts of material to be placed in the beam. This problem is of special interest during normal beam operation as any

significant increase in the beam size at Target T1 must be avoided. Calculations show (James 1972) that of the four locations at which monitors are to be placed during normal operation, only location 9 is suitable for the continuous operation of an intercepting monitor. These calculations indicate that up to 20 mg/cm^2 of aluminum (or its equivalent) can be placed anywhere within 25 cm of Target T1 without increasing the horizontal beam size by more than 40%. The beam size in the y plane changes by less than 1%. Continuously operating, intercepting monitors should not be used at points 2,5, or 8 as they would result in large increases in the beam size at T1 and in some cases would cause the acceptance of the transport system (notably quadrupoles Q7 and Q8) to be exceeded. For example, a 1 mg/cm^2 Al foil placed at 8 would increase the horizontal size of the beam at T1 from 50 to 100% depending on the energy of the beam. Note, however, that there is no objection to using intercepting devices at any location if provision is made for there extraction from the beam during periods when experiments are to be run.

Amongst the other problems associated with the development of the various monitors are the limitations on their size. Because of large beam sizes expected during beam alignment (see Table 3.4) the monitors used for this purpose should all have apertures of the order of 3 to 4" in diameter. This is also true of the devices used at points 5 and 8 during normal operation. A 1" aperture is sufficient at points 2 and 9 as the maximum beam widths expected at these points

are of the order of ½ cm. In the case of the monitors at 1 and 9, spatial limitations and shielding requirements restrict the total size of the device along the beam line to 10 to 15 cm. Between the combination magnet and quadrupole Q1, i.e. location 1, space must be allowed for vacuum flanges as well as for a vacuum shut-off valve.

Problems associated with radiation damage and heat dissipation strongly depend upon the type of monitor and will be discussed in subsequent chapters. The devices used should be reliable because of the limited access to the beam lines and because many locations will be inclosed in shielding. Where possible the electronics associated with these devices should be located outside the beam line shielding as this would facilitate easy servicing and replacement, and would protect them from radiation damage. Table 3.5 presents a summary of the monitor locations to be used, the parameters to be measured at each location, the purposes that these measurements will serve and the resolution required in the various measurements.

T A B L E 3.5

Summary of the Monitor Requirements Along the First Section of Beam Line I

Location	Type of Monitor	Purpose	Required Resolution Low Intensity	High Intensity
1	Position	Locate stripping foil. Set combination magnet.	1.0 mm	------
	Intensity	Measure extracted beam intensity.	1.0 nA	------
2	Position	Locate stripping foil. Set combination magnet.	1.0 mm	3-5 mm
	Intensity	Measure beam spill up to magnet B2.	1.0 nA	1.0 μA
	Profile	Measure energy spread. Optimize quadrupole current settings.	1.0 mm	3-5 mm
3	Position	Locate stripping foil. Set combination magnet.	2.5 mm	------
	Intensity	A Faraday cup located here could be used to calibrate relative intensity monitors.	1 nA	------
4	Position	Set 20° bending magnet.	1.0 mm	------
	Intensity	Measure beam spill in bending magnet.	1.0 nA	------
5	Position	Set 20° bending magnet.	1.5 mm	3-5 mm
	Intensity	Measure beam spill up to quadrupole Q6.	1.0 nA	1.0 μA
	Profile	Measure emittance. Optimize quadrupole current settings.	1.5 mm	3-5 mm
6	Position	Set steering magnets S1 and S2.	1.0 mm	------
7	Position	Set steering magnets S1 and S2.	1.0 mm	------

T A B L E 3.5 (cont'd)

	Profile	Measure emittance.	1.0 mm	------
8	Position	Check steering of quadrupoles Q7 and Q8.	1.5 mm	3-5 mm
	Profile	Locate waist near Target T1. Optimize quadrupole current settings.	1.5 mm	3-5 mm
9	Position	Measure beam position at Target T1.	0.2 mm	0.5 mm
	Intensity	Measure current hitting Target T1.	1.0 nA	1.0 μA
	Profile	Measure size of beam hitting Target T1.	0.2 mm	0.5 mm/0.5 cm
10	Profile	Locate waist near Target T1.	1.5 mm	------

CHAPTER 4

BEAM INTENSITY MONITORS

4.1 The Faraday Cup

The Faraday cup is a device in which the total beam is stopped and the deposited charge is measured using a calibrated capacitor; it usually takes the shape of a Faraday cage. It has been found to be the best available absolute intensity monitor since it essentially depends on the accurate measurement of collected charge. Several authors have reported absolute accuracies of 0.5% or better, although in the case of high energy proton beams accuracies of a few percent are more usual (Willard and Riley 1971). While the initial testing may in some cases be tedious, the calibration of the monitor at any given energy never changes except possibly as a result of changes in leakage currents, which can readily be checked. For a given energy, the calibration is linear as a function of beam intensity. Since the charged particles in the beam must be collected, the cup must be large enough to stop the beam and contain the secondary reaction products. As a result there is an upper energy limit for the usefulness of a given cup design. The maximum intensities that can be measured are set by power dissipation and leakage current limitations. The SLAC Faraday cup (Yount 1967, 1968), which is used to monitor the 20 GeV electron beam, has been operated at long-term and short-term power levels of 1 kW and 10 kW, respectively, without the aid of water-cooling. The water-cooled cup shown in

Fig. 4.1 is presently being designed at LAMPF (Willard and Riley 1971) for use with 100-800 MeV proton beams at currents up to 5 μA. This represents a maximum power dissipation of 4 kW, well below the 225 kW of the TRIUMF proton beam at full power. It is still sufficient for the Faraday cup to be used as a primary standard for testing and calibrating other monitors over a significant intensity and energy range. Such a cup could be used continuously in the proton area at TRIUMF, where accurate intensity measurements are required for cross-section measurements, as the maximum power of beams transported to that area is 5 kW (10μA at 500 MeV). As for the minimum measurable intensity, Grossetête and Isabelle (1968) have reported measuring the average intensity of a 10^{-2} nA, 1.3 GeV electron beam to within 1%. This is well below the 1 nA minimum threshold suggested for TRIUMF proton beam monitors.

There are several problems which must be overcome in designing a Faraday cup. The cup must be large enough to stop essentially all of the beam, and as the particle energy increases this is an increasingly difficult problem. In the past, empirical formulas introduced by Brown and Tautfest (1956) have been used with success to determine the minimum dimensions required for a Faraday cup used to monitor electron beams. These formulas were based on the work of Kantz and Hofstadter (1952, 1954) concerning electron-induced showers in various materials. More recently, the Monte Carlo calculations of Nagel (1965) and Völkel (1965) have been

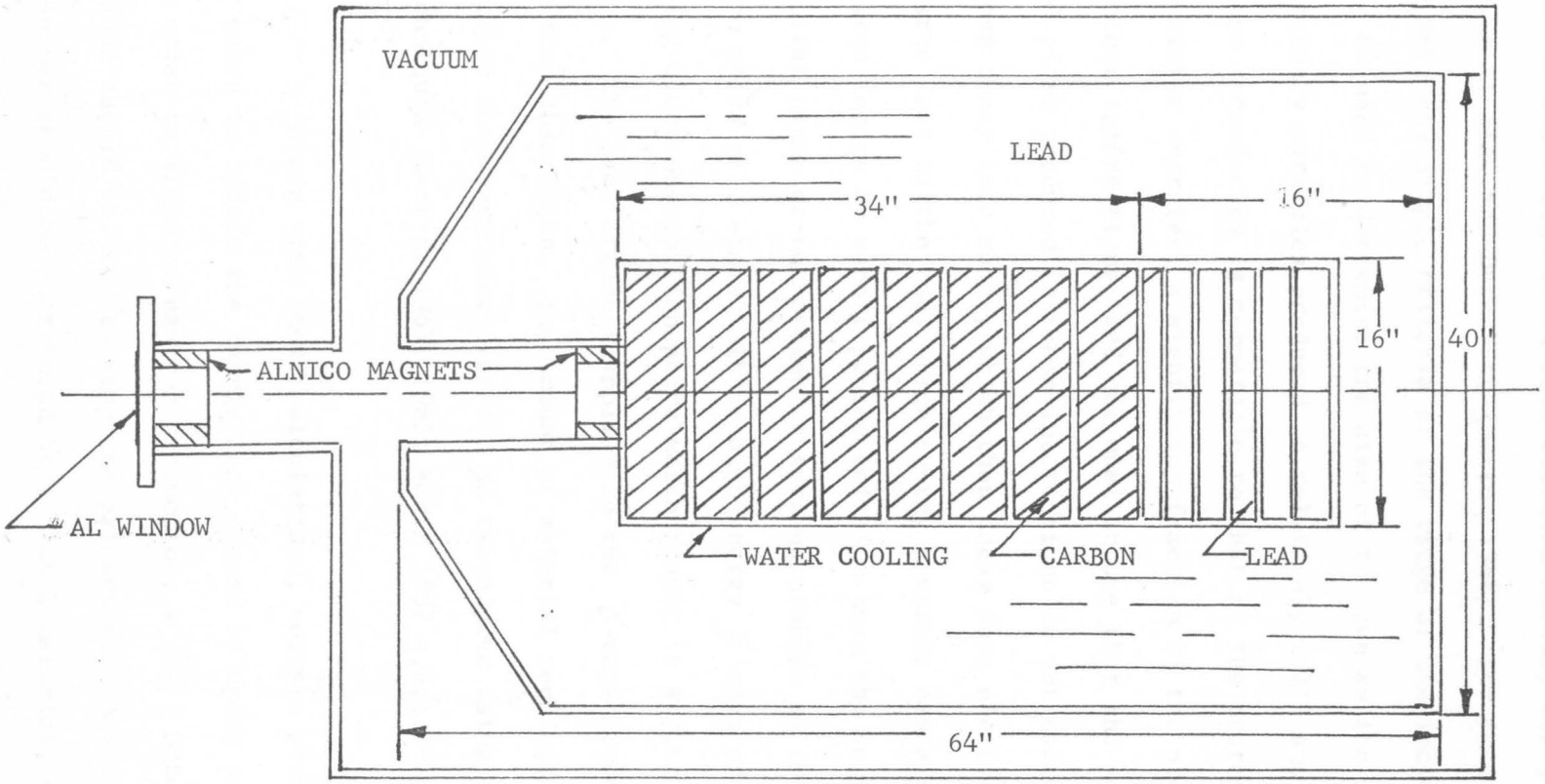

Fig. 4.1 The LAMPF 800 MeV Faraday cup

used in the design of several electron Faraday cups, including those at SLAC and Daresbury (Hatton 1968). For proton beams below 50 MeV, the simple criteria of the range of the incident protons can be used to determine the size of the cup as the number of secondary particles produced is relatively small and the range of these secondaries is comparable to that of the proton beam. However, at higher energies, a significant fraction of the protons undergo nuclear interactions, and one must insure that the scattered protons and pions produced in these interactions do not escape. Charged pions decay into muons, which then decay into electrons with possible charge loss to the cup. High energy neutrons can also give rise to charge losses by recoil proton emission near the surface of the cup. Neutral pions do not present a serious problem as they decay rapidly into pairs of γ-rays. These high energy γ-rays produce forward going electron-position pairs which result in a very small net charge loss. The same argument applies to the γ-rays produced by thermal neutron absorption. The amount of material required to stop these various secondary particles can be calculated using Monte Carlo techniques (Bertini 1963, 1965; Ranft 1967 a,b,; 1970).

Along with these calculations, certain precautions can be taken to reduce the charge loss caused by these secondary particles. In order to minimize neutron production, a low Z material such as carbon should be used to stop the primary proton beam. This proton absorber should be surrounded by a high Z material, several radiation

lengths thick, in order to reduce the number of pion and neutron interactions occuring near the surface of the cup. Lead or copper is commonly used for this purpose. In the case of cups built to stop electron beams, a jacket of low Z material, such as aluminum, is often placed around the lead in order to reduce the production of photoelectrons on the block surface. This may not be necessary in the proton case since the production of γ-rays will be much smaller.

A further problem associated with the design of a Faraday cup is the emission or collection of secondary electrons which would alter the measured charge. Secondary electrons will be produced at the entrance of the cup, and the current produced by such an effect can be as much as 3 to 4% of the incident current. The charge loss due to these secondary electrons is reduced by the Faraday cage structure which has the effect of making the mouth of the cup as small as possible. Such a design reduces the solid angle for the escape of these particles as well as for back-scattered primaries and reaction secondaries. In addition, the secondary electron loss can be reduced by using a magnetic field at that point where the beam enters the stopping material. A field of 250 gauss should be sufficient to trap all secondary electrons with energies below 1.5 MeV. The same magnetic field can be used to prevent secondary electrons produced in the entrace foil from reaching the cup. This entrance foil is required since the cup

must be evacuated in order to prevent the collection of charged particles arising from the ionization of gas molecules between the cup and its surroundings. A pressure of 10^{-3} Torr will reduce this effect to less than 0.1% (see equation 4.4.2).

In the presence of radiation, there are additional sources of error caused by ionization. For example, air spaces around electrical connections serve as a source of ions. This problem can be avoided by using a slide-back electrometer (Brown and Tautfest, 1956) to measure the charge on the Faraday cup, since this enables the cup and its connectors to be kept at ground potential. Such an electrometer also serves to reduce electrical leakage problems to a point where they are not important.

The major limitations on the construction of a Faraday cup for TRIUMF arise from its large size and high cost. It has been estimated that the cup being designed at LAMPF (Willard and Riley, 1971), which will be similar to that used at TRIUMF, will weigh 13 tons and cost $50,000. Because of these two factors, it is suggested that one of the beam dumps in the proton area be constructed so that it could be used as a Faraday cup. This has the advantages, in addition to reducing costs, that the dump already provides the necessary cooling and shielding.

4.2 Induction Current Monitors

The induction current monitor has been widely used for

several years in industry to measure high intensity currents. More recently, due to the necessity of measuring the intensity of particle accelerator beams in a nondestructive way, studies have been carried out at several laboratories regarding the possibility of using such a monitor with relatively low intensity, short pulse length beams.

The monitor is essentially a transformer in which the beam forms the primary and a pickup coil would on a high permeability toroid forms the secondary. It is a nonintercepting device and can be calibrated by feeding a known current pulse through a separate calibration coil wound on the toroid. The signal induced in a symmetrically wound pickup coil is given by

$$e_i = \frac{k\,\mu_o a N}{2\pi} \ln\left(\frac{r_2}{r_1}\right)\frac{di_b}{dt} = \frac{L}{N}\frac{di_b}{dt} \qquad (4.2.1)$$

where

$k = \mu/\mu_o$,

r_1, r_2 = inside and outside radii of the toroid,

a = length of toroid along its axis,

i_b = instantaneous beam current,

N = number of turns in pickup coil,

L = self inductance of the toroid, and

t = time

Although this equation was derived using classical electrodynamics, it has been shown to be valid for relativistic particle beams (Bergere et al. 1962 a,b), with the result that the output is independent of beam energy. The output has also been observed to be independent of beam position, although a small ($\approx$ 2 to 3%) variation with beam position is seen if a nonsymmetrical winding is used. The coil inductance L should be chosen as a compromise between the fact that L must be as large as possible in order to have a large output signal, while the wiring capacitance and resistance must be kept small if the rise time of the output is to be short compared to the beam pulse width, which is of the order of 5 to 10 nsec for TRIUMF beams.

The major disadvantage of the toroid is its limited current range with most devices having a minimum sensitivity $>$ 1 μA peak current. Measurement of smaller intensities is difficult because of the small output voltages and noise limitations. A review of the most important sources of noise is given in a paper by Zulliger (1964). They include inhomogenous magnetic fields, R.F. Pickup, electrostatic pickup from the mains which can be quite large if pulsed equipment such as a spark chamber is in use, and electrostatic pickup from the beam itself. Extensive electrostatic and electromagnetic shielding is usually required to reduce the noise due to these sources to an acceptable level. The small surface area of the pickup coil serves to reduce noise caused by the

collection of charge particles, a problem which can be quite severe in several other types of monitors; e.g. electrostatic induction electrodes. Other problems arise because of inhomogenities in the toroid material as well as changes in its properties due to temperature variations and exposure to radiation. Grossetête and Isabelle (1968) report a 20% decrease in the permeability of their toroid after an exposure to a dose of 5×10^6 rad over a period of 1500 hrs. These problems can be reduced by using a toroid constructed with wrapped sheets of permalloy metal (e.g. Ultraperm 10) rather than a ferrite material; by monitoring the signal produced in two pickup coils wound on the toroid in opposite directions (Hohback and Mango 1967); and by calibrating the device at regular intervals. A feedback technique such as that suggested by Yamada (1962) can also be used to produce a signal which is independent of small changes in the toroid properties.

There are two basic methods by which a toroid can be used to measure beam intensity or charge. One method is to terminate the toroid in a resistance so as to develop a voltage proportional to the instantaneous beam current. When short pulse length beams are being measured, this is usually accomplished by connecting the toroid directly to coaxial cable which is terminated in its characteristic impedance, R, as shown in Fig. 4.2. The circuit has the advantage of a short risetime (1-2 nsec), and permits the output to be measured at a location remote from the toroid where radiation damage to amplifiers is not a problem. The voltage

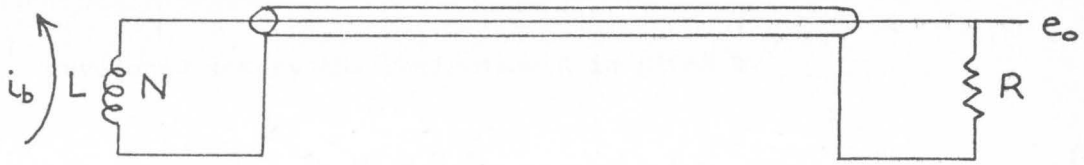

Fig. 4.2 A passive transformer

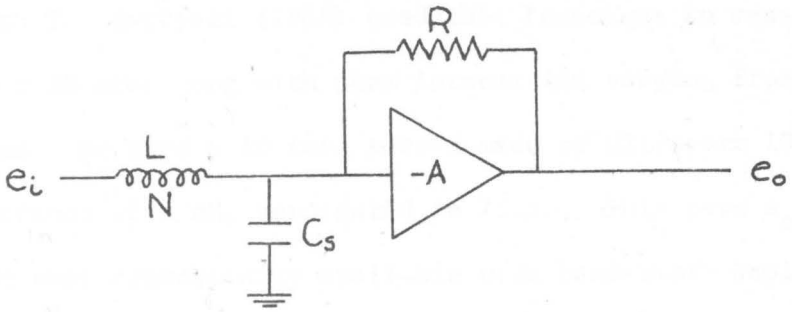

Fig. 4.3 The "Hereward" transformer

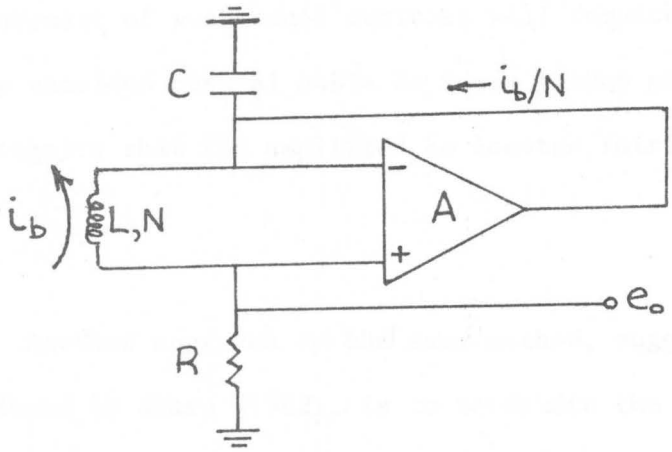

Fig. 4.4 A beam current transformer with DC to 200 MHz range

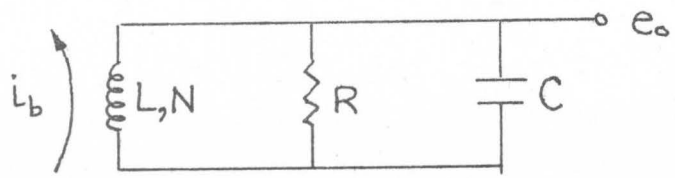

Fig. 4.5 A resonant tuned circuit transformer

developed across the resistance R is given by

$$e_o = \frac{R}{N} i_b \qquad (4.2.2)$$

provided the time constant L/R is much greater than the beam pulse length T. Battisti (1966) used this technique to measure beam pulses 10 nsec long with peak intensities varying from 400 μA to 800 mA. He used a 10 turn toroid made of Ultraperm 10 with an inductance of 5 mH, terminated in 75 Ω. This gave $e_o/i_b = 7.5\ \mu V/\mu A$. Given that commercially available wide band-width amplifiers have input noise levels of $\sim 1\ \mu V$, one should be able to detect peak currents of the order of 1 μA to 10% accuracy using this method. The measurement of such small currents will require the use of specially shielded coaxial cable to avoid pickup problems, and may in fact require that the amplifier be located fairly close to the toroid.

Another approach to the same method, suggested by Hereward and developed by Sharp (1962), is to terminate the pickup coil in a low impedance, resistive feedback amplifier as shown in Fig. 4.3. The output is again given by equation 4.2.2, provided

$$\frac{RC_s}{A} \ll T \ll \frac{LA}{R} \qquad (4.2.3)$$

where C_s is the stray capacity of the coil and the cable connecting the toroid and amplifier. This circuit can only be used for measuring long pulse length ($T > 0.5$ msec), low frequency beams since phase shifts in the feedback loop cause instabilities at high frequencies. Even for these beams, peak currents of the order of 10 μA are very difficult to measure using this circuit (Sharp 1962, Zulliger 1964).

Unser (1969) has since developed a circuit with DC to 200 MHz range based on the principle of the Hereward transformer. The basic circuit is shown in Fig. 4.4. The L/R integrator of the previous circuit is restricted in high frequency response by stray capacity C_s and by the slewing rate limit of the operational amplifier A. Unser uses coaxial cable terminated in a resistance R to eliminate the effect of C_s and thereby conserves the risetime of the passive transformer. Amplifier A acts to maintain a low impedance ($\sim 1\Omega$) across the secondary of the toroid, and also supplies current to drive the load resistor, R. The initial response of the circuit is determined by R,L, and C, and is independent of the amplifier. Therefore the amplifier need not have a wide bandwidth, resulting in a reduction of the problem of stabilization. The value of R is limited only by the stray circuit capacitance, which acts to limit the risetime of the system. The output is again given by equation 4.2.2.

For a 10 turn coil and R = 50 Ω , Unser (1969) reports a useable dynamic range of 100 μA to 1 A, while a prototype built at LAMPF (Trump 1971) is reported to have a resolution of 1 μA; this limit being set by 60 Hz pickup. Unser measured a risetime of 1.7 nsec using this circuit. At LAMPF, the long pulse lengths (500 μsec) permitted the designers to use a 1 kΩ resistor and a 50 turn coil, given a sensitivity of 20 μV/μA.

The second basic method used to measure beam intensity is to load the toroid with a capacitor so as to cause it to resonate when a pulsed current passes through the core. In this manner, a low frequency voltage proportional to the beam charge is developed at the toroid terminals; the waveform is then amplified and sampled at one of its peaks to obtain a measure of the beam pulse charge. The theory of operation and the circuits used to sample this output are described in several reports (Olsen 1965; Larsen and Horelick 1968, 1969; Larsen 1971). The basic circuit is shown in Fig. 4.5, where R is a damping resistor and C is the required capacitance. Adapting this technique to a synchronous cyclotron beam is difficult because of the high repetitive frequency of the beam pulses and the low peak beam intensity. For this type of accelerator it is more common to use a tuned circuit technique in which the capacitor C is used to tune the sensor circuit to the beam pulse repetition frequency or one of its higher harmonics. Assuming that the cyclotron beam current can be represented by a periodic series of

rectangular pulses of magnitude I_b, duration T and period τ, the Fourier series for such a current is

$$i_b = I_b\left[\frac{T}{\tau} + \frac{2}{\pi}\sum_{n=1}^{\infty}\frac{1}{n}\sin\frac{n\pi T}{\tau}\cos\frac{2n\pi t}{\tau}\right] \qquad (4.2.4)$$

The voltage induced in the sensor circuit is from equation 4.2.1.

$$e_i = \frac{-4LI_b}{N\tau}\sum_{n=1}^{\infty}\sin\frac{n\pi T}{\tau}\sin\frac{2n\pi t}{\tau}$$

By tuning the circuit to the n=1 mode, the voltage developed across the capacitor is

$$e_o = -\left[\frac{4LQ}{N\tau} I_b \sin\frac{\pi T}{\tau}\right]\sin\frac{2\pi t}{\tau} \qquad (4.2.5)$$

where Q is the quality factor of the circuit. This voltage is amplified and used as a measure of the peak current I_b.

This technique has been used by Johnson and Ramler (1963) for monitoring the external Argonne National Laboratory (ANL) cyclotron beam for a current range of 30 nA to several microamps. They, however, used very expensive, high gain ($\sim 10^6$), low bandwidth amplifiers designed to amplify the cyclotron's fundamental frequency of 11.2 MHz. In spite of the higher current sensitivity of this technique compared to those already discussed in this section, the high cost of the amplifiers may prohibit the use of this method for monitoring TRIUMF's proton beams.

4.3 Electrostatic Beam Monitor

A second type of nonintercepting beam monitor is the electrostatic pick-up electrode. In its simplest form it consists of a metallic cylinder of length W, having a capacitance to ground C, which is traversed by a particle beam of average intensity i_b and charge q. The basic geometry is shown in Fig. 4.6. The voltage induced on the pick-up electrode is given by

$$V = \frac{1}{C}\int_o^W dq = \frac{1}{C}\int_o^W i_b \frac{ds}{\beta c} = \frac{W i_b}{\beta c C} \qquad (4.3.1)$$

where the capacitance is given by (neglecting and effects)

$$C = \frac{2\pi \epsilon_o W}{\ln (b/a)} \qquad (4.3.2)$$

The output voltage is therefore independent of W; however from a current and capacitance point of view W should be as large as possible. To maximize the output voltage V, the ratio b/a should be large. At TRIUMF these dimensions have the following limitations at most monitor locations (see Section 3.6): $W \leq 30$ cm, $a \geq 5$ cm, and $b \leq 15$ cm. For $b/a = 3$ and $W = 30$ cm, $C = 15$ pf and the sensitivity V/i_b is 100 $\mu V/\mu A$, which is of the order of 10 to 100 times larger than the sensitivity of the toroid. This sensitivity will probably be reduced to ~ 50 $\mu V/\mu A$ because of the capacity of feedthroughs and connections to the electrometers used to measure the output. These electrometers should be mounted directly on the monitor box to reduce this effect. This may pose a problem because of the high radiation levels.

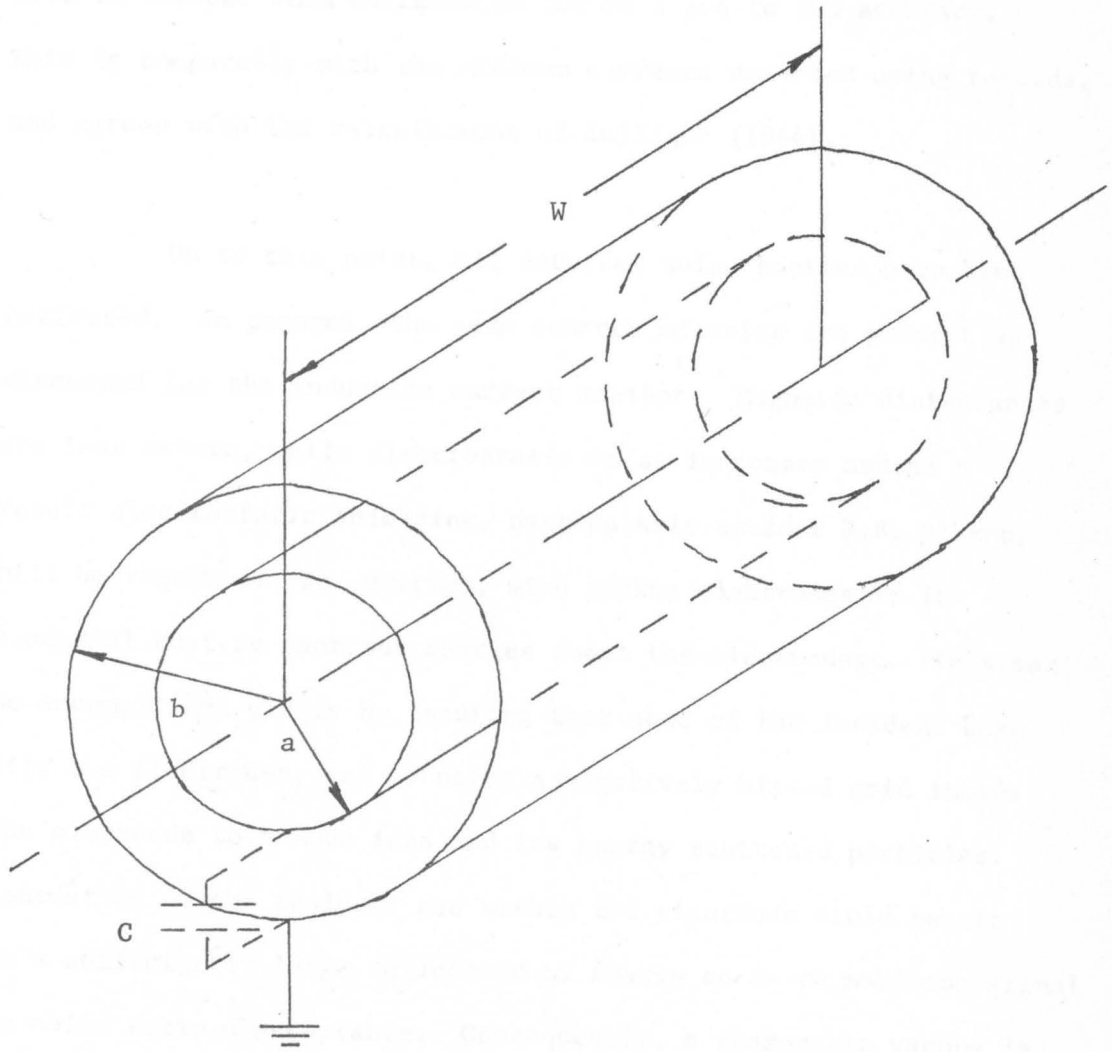

Fig. 4.6 A typical electrostatic beam monitor

The minimum current measurable is set by the noise levels of the electrometer tubes. Typically such electrometers have current noise levels of the order of 10^{-15} A and input impedances of 10^{10} Ω. Using these values and a sensitivity of 50 μV/μA, one should be able to measure beam currents as low as 2 μA to 10% accuracy. This is comparable with the minimum currents detected using toroids, and agrees with the calculations of Zulliger (1964).

Up to this point, all external noise sources have been neglected. In general, the same sources of noise are present as discussed for the induction current monitor. Magnetic distrubances are less severe, while electrostatic noise increases and as a result electrostatic shielding, particularly against R.F. pickup, will be required. In addition, with pickup electrodes it is essential that no spurious charges reach the electrodes. This can be accomplished partly by insuring that none of the incident beam hits the electrodes, and by using a negatively biased grid inside the electrode to remove ions and low energy scattered particles. Ionization of the residual gas within the electrode could result in a sufficiently large collection of charge so as to make the signal to noise ratio unacceptable. Consequently, a reasonable vacuum is required. The pressures expected in the TRIUMF beam lines of less than 10^{-3} Torr are adequate, since a 500 MeV proton beam produces only 10^{-1} ion pairs per proton per Torr per cm of path length in air.

One disadvantage of this device is that its output is energy dependent ($V \propto 1/\beta$). In contrast to the toroid, the electrostatic monitor is not self calibrating and the calibration must be done against some other type of current monitor. As the Faraday cup envisioned for TRIUMF will be designed for a maximum intensity of 10 μA, it does not seem reasonable that it could be used to calibrate either the electrostatic device or the toroid. Since the electrostatic monitor has a maximum sensitivity of 1 μA average current, it could only be used during high intensity operation.

4.4 Ionization Chambers

One of the earliest devices developed for monitoring particle beams is the ionization chamber. A detailed description of the device and its operating characteristics is given by Fulbright (1958). Basically the monitor consists of an enclosure containing a gas in which the ionization is produced, and having two or more electrodes between which an electric field is applied so as to collect the resulting ions. To insure that all the ions are collected, field gradients of the order of 200 V/cm or more are usually required. For monitoring particle beams the monitor usually takes the form of a parallel plate ionization chamber, with the plates serving as vacuum windows to isolate the chamber from the residual gas in the beam lines. The available ionization current is given by

$$i_s = \frac{\rho d}{W}\frac{dE}{dx}\, i_b = \frac{P}{RT}\,\frac{d}{W}\,\frac{dE}{dx}\, i_b \qquad (4.4.1)$$

where ρ is the gas density ($\rho = P/RT$), d is the plate separation, W is the energy required to produce an ion pair ($\sim$ 35 eV for air), dE/dx is the energy loss of the beam in the gas (2.4 MeV/gm/cm^2 for 500 MeV protons in air), and i_b is the average beam current. For 500 MeV protons incident on air at standard temperature (T = 293° K)

$$i_s/i_b = 0.11/\text{cm Torr} \qquad (4.4.2)$$

That is, a 100 μA, 500 MeV proton will produce 8.4 mA of ions and electrons along each cm of its path in air at atmospheric pressure (760 Torr). The large signal amplification produced is the main advantage of the ionization chamber and permits the measurements of very small beam intensities ($< 10^5$ particles/sec). As seen from equation 4.4.1, i_s is directly proportional to i_b; however, at large beam currents many of the ions and electrons recombine to form neutral atoms because of the high ionization density in the gas, with the result that the response of the chamber becomes nonlinear. The value of the incident current beyond which the response is no longer linear depends on the beam current density, gas pressure, plate separation and voltage gradient used. By reducing the gas density and the plate separation, it is possible to construct a linear device for current densities up to 1 mA/cm^2. Several chambers have been used for measuring incident proton beam current densities ranging from 1 nA/cm^2 to 1 mA/cm^2 using air as the chamber gas. Better performance has been reported with gases such as argon, methane, and argon-carbon dioxide mixtures.

The accuracy of the ionization chamber depends mostly on the purity of the gas, the maintenance of a constant pressure, and the elimination of the effects due to recombination and secondary electron emission. The secondary electrons are produced in the vacuum windows and result in a current equal to approximately 2% of the beam current (see Section 4.5). Secondary emission is therefore important only at low pressures (< 10 Torr). For example, in a 10 cm long ionization chamber filled with air at a pressure of 10 Torr, $i_s = 11\ i_b$ and secondary electron emission from the windows contributes less than 0.2%. On the whole, accuracies of the order of 1% seem to be obtainable with several authors reporting an accuracy of 0.1% over a limited intensity range (e.g. Grossetête and Isabelle (1968).

Because of the high current densities (~ 1 mA/cm^2) and the small gas vacuum loading permitted on the beam line vacuum system, any ionization chambers used at TRIUMF will require fairly substantial vacuum windows, or a costly differentially pumped isolation section. Calculations done by Hodges (1971) on the thin windows in intense proton beams suggest the use of 0.001" (26 mg/cm^2) molybdenum foils for windows. Thinner windows suffer from fatigue and are not vacuum tight. For continuous monitoring, an ionization chamber therefore offers more scattering material (> 50 mg/cm^2) than desired to the beam, and insertable chambers must be used.

The residual gas in the beam line may be used to produce the ions, dispensing with the need for windows. However, in the section of line up to Target T1 the pressure in the line is expected to be less than 10^{-6} Torr, so the sensitivity of the device is not sufficient. This procedure can be used downstream of T1 where vacuum line pressures are permitted to be larger ($\sim 10^{-3}$ Torr), although accurate pressure measurements are required.

The ionization chamber appears to be a suitable monitor for measuring the beam intensity at TRIUMF, especially during beam alignment when small intensities must be measured. It cannot be used continuously to monitor the high intensity (100 μA) beam at points upstream of T1 because of multiple scattering. Downstream of T1 this should not be a problem. Some recombination effects may be seen at the larger intensities, especially where the beam profile is small. The ionization chamber can also be used as a crude beam spill monitor by placing it at points near the beam line.

4.5 Secondary Emission Monitors

The use of secondary emission as a means of measuring the intensity of incident radiation arose out of studies of the saturation properties of ionization chambers (Taylor 1951; Greening 1954; Wilson 1954). It was during these studies that the phenomena of secondary emission was found to occur in ionization chambers when extrapolation of the x-ray or γ-ray currents to zero pressure

resulted in a non-zero current, in disagreement with the Bragg-Gray theory. The first Secondary Emission Monitor (SEM) designed specifically to monitor high energy beams of charged particles was constructed by Tautfest and Fechter (1955) at Stanford University. Since then most nuclear physics laboratories possessing a particle accelerator have constructed their own SEM's, including several high energy proton accelerator facilities (Harting et al. 1960; Agoritsas 1968; de Parry and Ratner 1969).

The SEM operates on the principle of the emission of secondary electrons from material on passage of a high energy beam of charged particles. As shown in Fig. 4.2, it consists of a set of thin foils alternately phased in voltage. The current resulting from the secondary electrons produced in these foils is collected on one set of the foils, and is measured using a calibrated capacitor or an electrometer. The ratio of this current to the primary beam intensity is defined as the yield or efficiency of the SEM and, as shown in Tables 4.1 and 4.2, it is of the order of 2 to 4% per emitting surface. The yield has been found to remain constant for beam currents ranging from 10 pA to 1 mA (Harting et al 1960; Taimuty and Deaver 1961; Okabe et al. 1961). The SEM is free from the saturation problems found in ionization chambers and has been used at current densities up to 150 mA/cm^2 (Taimuty and Deaver 1961; Agoritsas 1968), which is well above the levels to be found at TRIUMF. The SEM must be operated at pressures less than 10^{-3} Torr

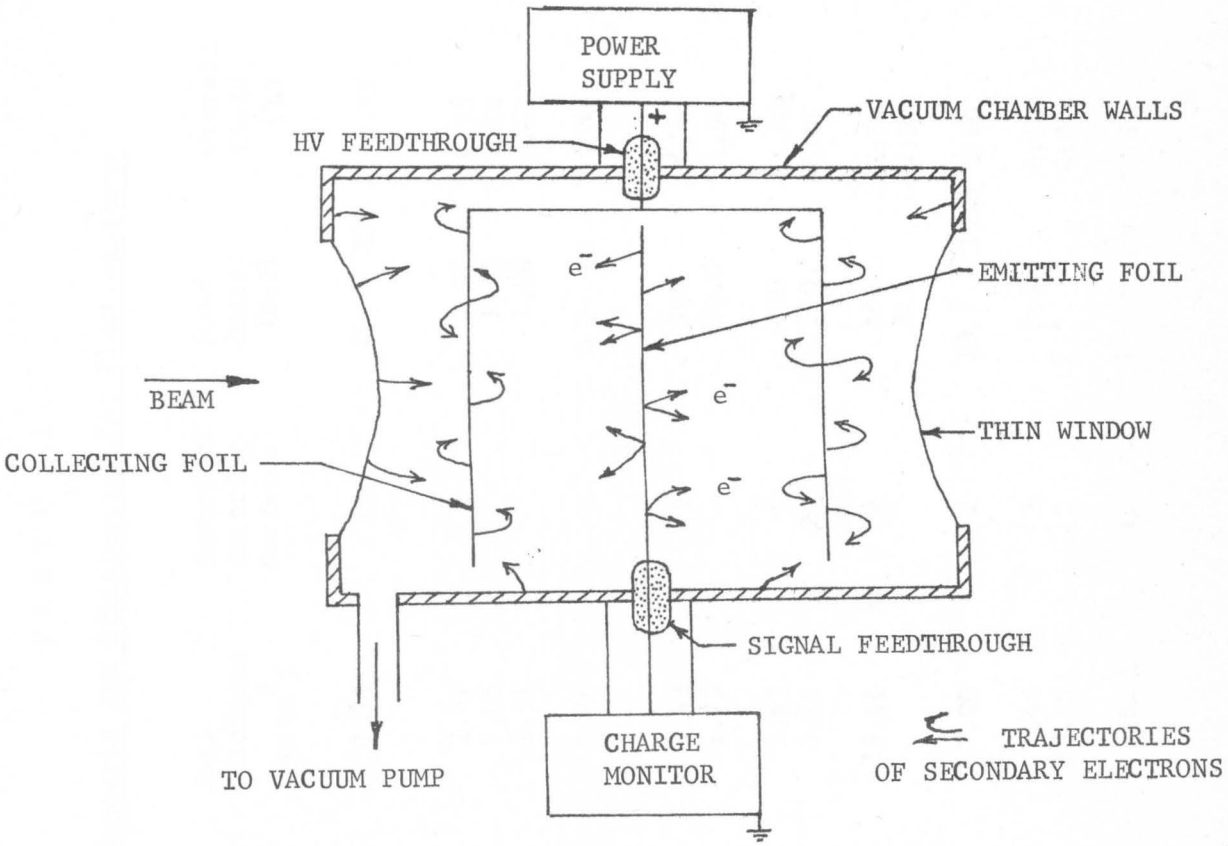

Fig. 4.7 Principles of a secondary emission monitor

T A B L E 4.1

Reported SEM Efficiencies For Electron Beams

Reference	Foil Material	Foil Thickness (mg/cm^2)	Number of Emitting Surfaces	Beam Energy (MeV)	Overall Yield (%)	Yield per Emitting Surface (%)
Tautfest Fechter (1955)	Al	1.71	19	111 - 235	39.75	2.09
Vanhuyse et al. (1962)	Al	2.62	2	2.00	4.35	2.17
		2.05		1.75	4.14	2.07
		1.51		1.60	3.15	1.57
Taimuty and Deaver (1961)	Al	2.06	2	6 - 30	5.00	2.50
Vanhuyse and Van de Vijer (1962)	Al	3.43	2	200	4.00	2.00
		1.73		30.0	2.94	1.47
Isabelle and Roy (1963)	Al	1.62	6	230	12.00	2.00
		3.24	20	150	44.00	2.20
	Al & Au	15.66	6	144	22.80	3.80
				215	24.00	4.00
Planskoy (1963)	Al	7.00	2	10.7 - 15.3	3.80	1.90
Okabe et al. (1963, 1964)	Al	1.40	3	7.5	6.60	2.20
	Au	38.00	2	7.5	4.00	2.00
Ladage and Pingel (1965)	Al	1.62	16	1 - 5 Gev	51.8	3.23

TABLE 4.2

Reported SEM Efficiencies For Proton Beams

Reference	Foil Material	Foil Thickness (mg/cm^2)	Number of Emitting Surfaces	Beam Momentum (GeV/c)	Overall Yield (%)	Yield per Emitting Surface (%)
Harting et al. (1960)	Al	5.40	19	1.21	54.00	2.84
Michaelis and Hirt (1960)	Al	5.40	19	1.21	34.70	1.83
Agoritsas (1968)	Al	1.35	4	7.00	7.29	1.82
				8.00	7.48	1.87
				9.00	7.49	1.87
				10.00	7.62	1.90
				11.00	7.64	1.91
				12.00	7.87	1.97
				16.70	8.49	2.12
				19.20	8.50	2.12
de Parry and Ratner (1969)	Al	3.34	14	3.6	37.8	2.70
				4.4	37.8	2.70
				4.7	38.2	2.73
				6.4	38.6	2.76
				7.1	39.1	2.79
				7.6	40.2	2.87
				8.45	39.6	2.83
				9.0	40.6	2.90

in order to reduce the effect of the ionization of residual gases. From equation 4.4.2, 10^{-4} ion pairs are produced per proton per centimeter of path length in air at 10^{-3} Torr by a 500 MeV proton beam. Given that the SEM foils are separated by 1 cm and that all the ions are collected by these foils, the resulting current would amount to only 1% of the secondary electron current.

Accurate calculations of the secondary emission yield cannot as yet be made as the basic mechanism and the effect of the foil surface conditions, are not well enough understood. A derivation given by Tautfest and Fechter (1955), based on the scattering of atomic electrons by protons according to the Rutherford formula, is not complete as this treatment fails to explain the very low average energy of the secondary electrons which has been found experimentally.

An estimate of the yield can, however, be made in the following way. When a beam of incident particles passes through one of the foils, a number of atoms along the path of the beam are ionized. This process is analagous to the ionization of gas atoms along the path of a high energy beam of charged particles. Electrons that have been liberated by the ionization process can escape from the foil if their energy is sufficiently large to overcome the surface barrier potential, and if they are produced near enough to the surface. If the velocity of the incident particles is

much higher than that of the atomic electrons, the yield can be written as (Harting et al. 1960; Aggson 1962)

$$Y = k \frac{dE}{dx} \tag{4.5.1}$$

where dE/dx is the energy loss per gm/cm^2 of the incident particle in the foil material, and k is a constant approximately independent of energy but which depends markedly on the foil material and surface conditions. In Fig. 4.8, the experimental results of Agoritsas (1968), and de Parry and Ratner (1969) for high energy protons incident on aluminum SEM's have been plotted as a function of dE/dx for protons in aluminum, and they show good agreement with the above equation. Although no measurements exist for 200 to 500 MeV protons, measurements for electrons of the same velocities (Aggson 1962; Karzmark 1964) indicate that the yield should be proportional to dE/dx even at these proton energies.

The variation of yield with bias voltage applied between the two sets of foils in an SEM is shown in Fig. 4.9. The maximum in the yield at 30 volts suggests that nearly all of the secondary electrons have energies less than 30 eV and that they are emitted from the external molecular layers of the foils. These results support the theory that the majority of secondary electrons result from the ionization of the atoms within the foils.

A further less important process which contributes to the production of secondary electrons is the ionization of atoms in the

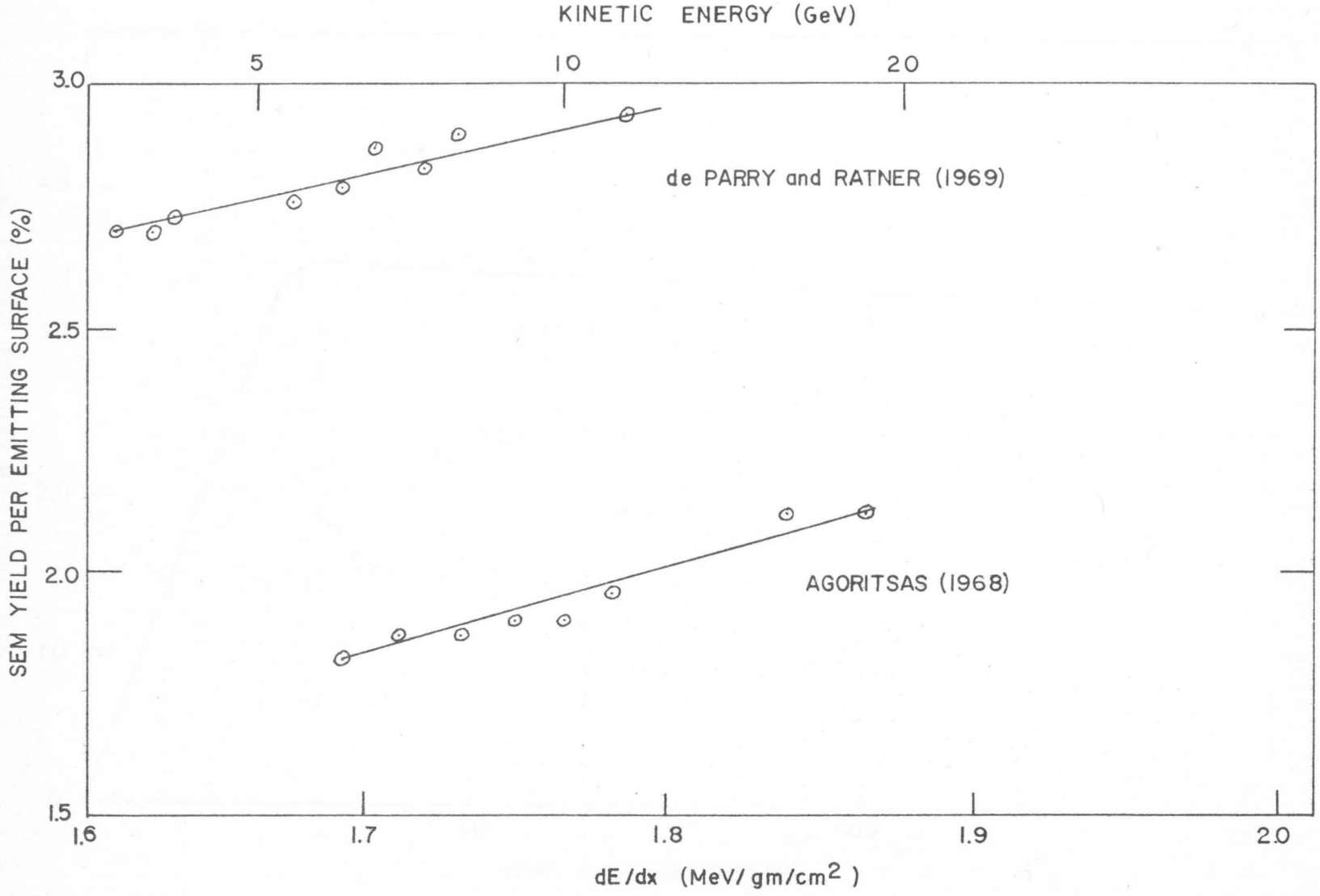

Fig. 4.8 Secondary emission yield as a function of kinetic energy and dE/dx for protons in aluminum

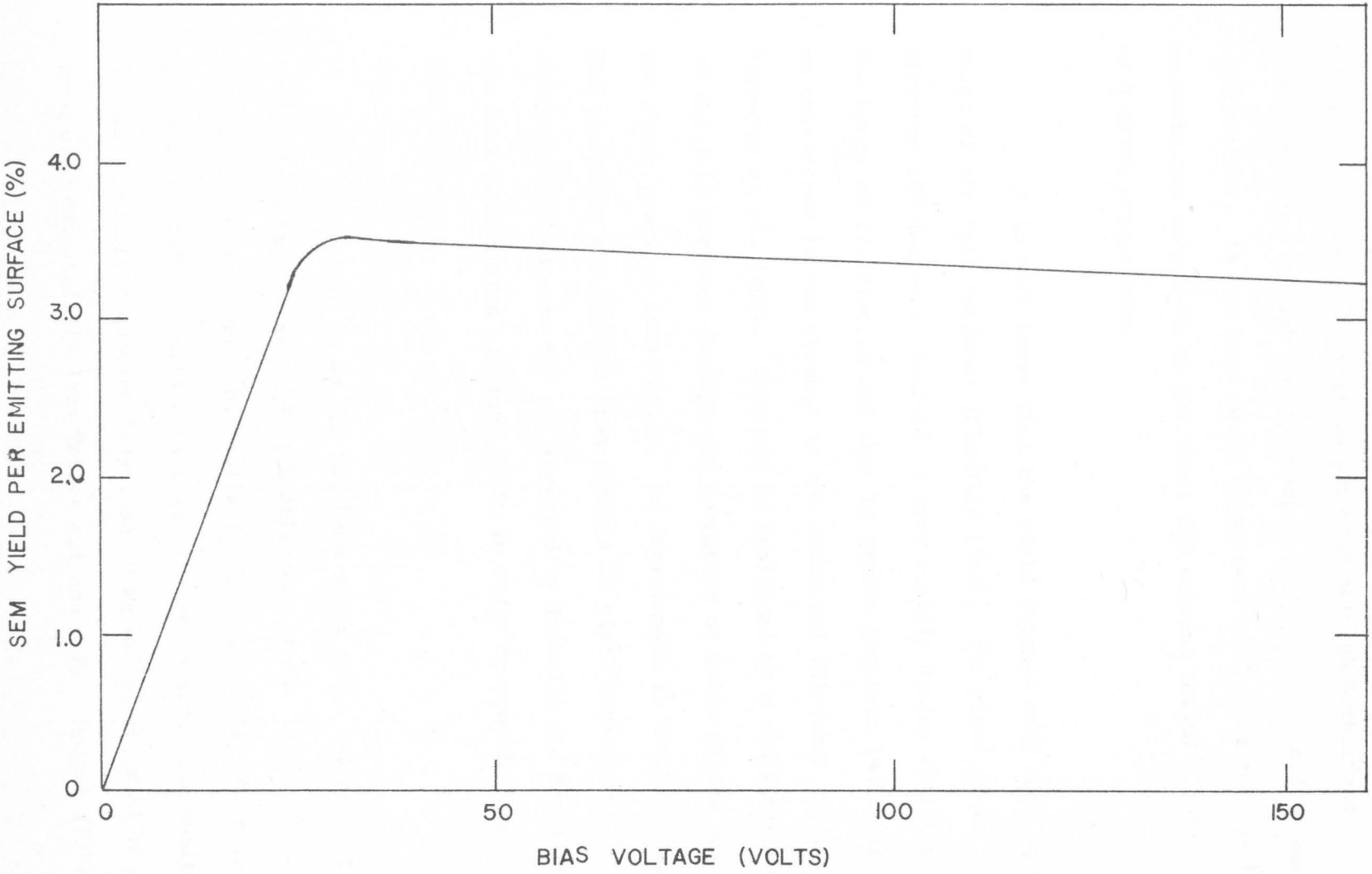

Fig. 4.9 A typical bias voltage curve for a secondary emission monitor

foil both by knock on electrons produced through Rutherford scattering, and by high energy charged particles produced by nuclear interactions. It has been shown (Agoritsas 1968) that this process accounts for only 2-3% of the total SEM current measured for a 19.2 GeV/c proton beam.

It is well known that the yield depends very much on the state of the foil surfaces (Planskoy 1963). The yield of an aluminum SEM has been observed to vary rapidly during the first few hours of irradiation and then to remain constant ($\pm$ 1%) as long as the vacuum in the chamber is not destroyed (Planskoy 1963; Vanhuyse et al. 1962). This can be explained by a modification of the foil surfaces through the formation of oxide layers during the first hours of irradiation. An improvement in the long term SEM stability and freedom from changes in yield immediately following exposure to air was reported by Isabelle and Roy (1963), who used gold-plated aluminum foils in order to provide a more stable foil surface.

The yield of an SEM has been shown to be independent of foil thickness (Planskoy 1963; Blankenburg et al. 1965). This permits the use of very thin foils (1 to 2 mg/cm^2 Al) which reduce the beam degradation effect of this type of intercepting monitor. Several monitors requiring less than 10 mg/cm^2 of material have been used successfully (see Tables 4.1 and 4.2). Hodges (1971)

has shown that conduction cooling of such foils is sufficient to prevent them from melting when exposed to the proton beams expected at TRIUMF.

The SEM can be used to monitor the TRIUMF proton beams over the full range of currents involved, subject to the limitations outlined in Section 3.6 regarding beam degradation. Measurements of the yield as a function of energy will have to be made against an absolute monitor because of the sensitivity of the efficiency to surface conditions. It may be necessary to supply the monitor with its own vacuum system in regions along the beam lines where the pressure exceeds 10^{-3} Torr, or where the vacuum must frequently be broken.

4.6 Monitoring Using Activation Techniques

Foil activation techniques have been used extensively for measuring the absolute intensity of accelerator beams (Cumming 1963; Caldwell 1961; Steinberg 1971). This method consists of measuring the induced activity of a sample of material exposed to the beam. In order to make such a measurement one must know the activation cross-section for the particular reaction used, the number of atoms in the foil, the counting efficiency, and the history of the exposed sample. Measurements made in this way can be done over a wide range of energies to ± 10%, but achieving accuracies much better than this is possible only at energies where the cross-section is well known. The determination of an absolute cross-section requires a measurement of the absolute flux of particles. This is

usually done by counting individual particles or by using a Faraday cup (Cumming 1963; Yuan and Wu 1961; Ritson 1961). Both of these methods are limited to accuracies of a few percent for proton beams of the energies in question. The most accurate cross-sections are rarely quoted to better than ± 3%. Table 4.3 lists the standard deviations for the most commonly used monitor cross-sections along with the pertinent radioactive properties of the nuclides involved (Steinberg 1971).

The major advantage of the activation technique is its linear dependence on beam intensity. It is a method which can be used for beams of all intensities, being limited only by saturation of the counters used to measure the activation. It is insensitive to the electric, magnetic, and photo environment. The technique does require that the beam be intercepted and cannot be used to continuously monitor the beam. In addition, the result is not immediately available as one must await the radioactivity analysis. The method is also subject to the effects of secondary particles and cannot differentiate amongst beam contaminants such as the high energy neutrons and pions found in proton beams. These various limitations prohibit the use of this technique along Beam Line I during normal operation. It is useful as a standard for calibrating monitors and for measuring beam intensities in experimental areas.

T A B L E 4.3

Nuclear Data for Nuclides Commonly Arising in Activation Measurements

Reaction	Cross-Section for 500 MeV Protons (mb)	Standard Deviation in the Cross-Section	Daughter Nuclide	Half-Life	Radiation	Natural Abundance
$C^{12}(p,pn)C^{11}$	30	5%	C^{11}	20.4 min	0.97 MeV β^+	1.00
$Al^{27}(p,5p,5n)F^{18}$	7.5	6.5%	F^{18}	110 min	0.635 MeV β^+	0.97
$Al^{27}(p,3pn)Na^{24}$	11	6.5%	Na^{24}	15 hr	1.39 MeV β^- 1.37 MeV γ 2.75 MeV γ	1.00
$C^{12}(p,3p3n)Be^{7}$	11	10%	Be^{7}	53.6 days	0.48 MeV γ	0.103
$A^{27}(p,3p3n)Na^{22}$	17	10%	Na^{22}	2.6 yrs	0.55 MeV β^+ 1.28 MeV γ	0.898

4.7 Other Intensity Monitors

Several commonly used intensity monitors exist which cannot be used for monitoring the proton beams produced at TRIUMF, but which may be useful in other applications such as measuring the intensity of TRIUMF's secondary beams.

The following single particle detectors are limited to counting the fluxes indicated: spark chambers, $< 10^2$/sec; geiger tubes, $< 10^3$/sec; proportional counters, $< 10^5$/sec; scintillation counters, $< 10^7$/sec. They therefore cannot be used to directly measure the intensity of TRIUMF's proton beams, but could be used as relative monitors by detecting particles scattered from a thin foil placed in the beam.

Nuclear emulsions, calorimeters and solid state detectors all require significant amounts of material to be placed in the beam. Nuclear emulsions must be exposed to less than 5×10^6 particles/cm^2 in order to retain accurate enough resolution so that the individual tracks may be counted, and therefore cannot be used in TRIUMF's proton beams. By their nature, emulsions cannot be used as continuous beam monitors.

Calorimetric procedures have seldom been used for either absolute (Marquez 1952) or relative (Prokoshkin and Tiapkin 1957)

intensity measurements in the energy range of interest because of the difficulties involved.

Solid state detectors are radiation sensitive and their output decreases rapidly with radiation over 10^{13} particles (Fabjan and Zulliger 1964).

Two techniques which are often used in monitoring electron beams are based on the emission of synchrotron radiation (de Raad, 1963) and Čerenkov radiation (Čerenkov 1937). As the intensity of synchrotron light is inversely proportional to the cube of the particle's mass, the amount of synchrotron light produced by high energy protons is far too small to be useful. Čerenkov light, which is produced when a particle traverses a material at a velocity greater than the velocity of light in the material, can be used to measure the intensity of high energy proton beams. However, at currents greater than 10^{7} particles/sec. the counter saturates and it cannot be used as an intensity monitor. Its use as a beam energy monitor is discussed in Chapter 6.

CHAPTER 5

BEAM POSITION AND PROFILE MONITORS

5.1 Electromagnetic Pickup Coils

As well as being used to measure beam current, the current transformer discussed in Section 4.2 has also been adapted to beam position measurements (Johnson et al. 1961; Bergère et al. 1962a; Johnson and Ramler 1963; Dorikens-Vanpraet et al. 1967). Two sets of detection coils are required to determine the horizontal and vertical co-ordinates of the beam position. Each set consists of two coils, connected in opposition and symmetrically placed about the mechanical centre of the beam pipe. The axes of the coils are aligned perpendicular to the direction of the beam and the direction to be sensed.

The voltage induced in each coil is given by

$$e_i = \frac{-2\mu AN}{r} \frac{di_b}{dt} \qquad (5.1.1)$$

where μ is the effective permeability of the coil-beam current flux loop, A is the cross-sectional area of the coil, N is the total number of turns on a coil, and r is the effective distance from the beam to the coil axis. If the beam is located symmetrically between the two coils, the voltage output will be zero. If it is displaced a distance Δr towards one of the coils, the output

will be

$$e_i = \pm \frac{4 \mu AN}{r^2} \frac{di_b}{dt} \Delta r \qquad (5.1.2)$$

The polarity of the output signal will depend on the direction of the displacement and along with the magnitude can be used to determine the beam position.

The most commonly used method for processing this output voltage in the case of cyclotron beams is the tuned circuit technique discussed in Section 4.2 (Johnson et al. 1961; Johnson and Ramler 1963). Several other techniques have also been used (Bergère et al. 1962 a,b,; Holcomb et al. 1963; Bergstrom 1963; Law and Holcomb 1965); however these methods are particularly suited to beams produced by linear accelerators which are usually characterized by peak current pulses of milliamps in magnitude and cycles/sec in repetition rate as compared to microamps and megacycles/sec for cyclotron beams.

Using the tuned circuit technique, Johnson and Ramler (1963) were able to measure the position of the external ANL cyclotron beam to an accuracy of ± 0.1 mm for beam currents down to 30 nA. The position accuracy decreased for lower beam currents. A derivation similar to the one used to derive equation 4.2.5 shows that the voltage developed across the tuning capacitor is

$$e_o = \pm \frac{16 \mu ANQ}{r^2 \tau} \Delta r \, I_b \sin \frac{\pi T}{\tau} \sin \frac{2 \pi t}{\tau} \qquad (5.1.3)$$

where I_b is the peak beam current, T is the beam pulse length, τ is the period between pulses and Q is the quality factor of the sensor circuit. From this equation Johnson and Ramler (1963) calculated the sensitivity $e_o/\Delta r I_b$ to be 40 μV/mm μA. The output thermal noise level was found to be 3 μV. Circuits of similar response could be built for use at TRIUMF although, as was the case at ANL, expensive high gain, low bandwidth amplifiers are required. This technique would therefore satisfy the position monitor requirements at TRIUMF; however it is expensive and could only be used for beam currents of the order of 10 nA or larger.

5.2 Electrostatic Pickup Electrodes

The electrostatic beam monitor described in Section 4.3 has also been adapted to beam position measurement. An example of this device is shown in Fig. 5.1, which was developed for the 20 MeV linear accelerator injector at the Lawrence Radiation Laboratory Bevatron (Allison et al. 1966). The electrodes are taken up in a resonant R.F. bridge tuned to the linac frequency. The beam position resolution with this particular system is of the order of $\pm$ 0.1 mm and a linear response with beam displacement has been observed. Several other electrode geometries have been used with similar position resolutions being measured (Sherwood

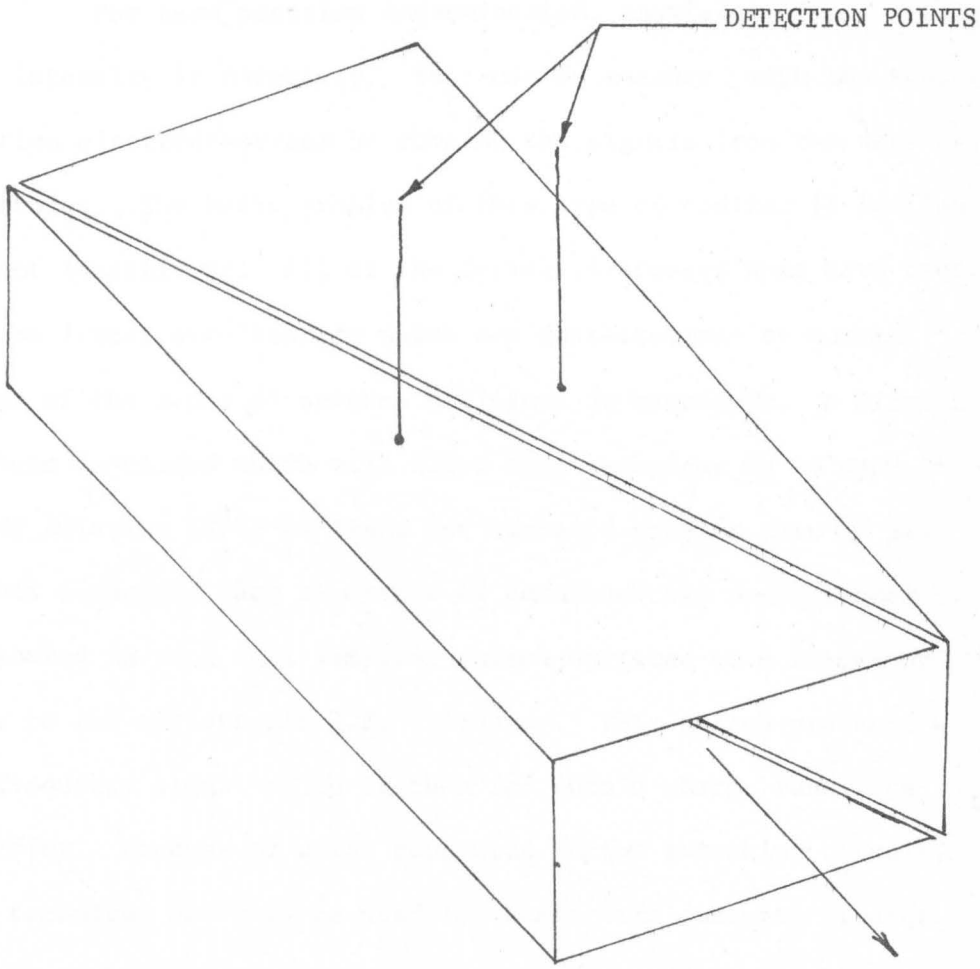

Fig. 5.1 A typical electrostatic position monitor

1965; Bogaards and Drake 1966; Simanton 1969). The longitudinal asymmetry of the electrodes shown in Fig. 5.1 eliminate phase shifts caused by beam transit time effects.

For beam position determination, knowledge of the total beam intensity is necessary. This can be measured with the above position electrode system by summing the signals from the various electrodes. The basic problem of this type of monitor is its low current sensitivity. All of the devices discussed here have been used on linear accelerators which are characterized by current pulses of the order of several milliamps in magnitude. A circuit has been developed which will allow this technique to be used at TRIUMF (Glavina 1971) at least for currents greater than 10 μA. In this technique each electrode is connected via coaxial cable terminated in 50 Ω to a sampling switch operated at a frequency close to the cyclotron's R.F. frequency. This switch produces a low frequency signal which is then fed into a charge sensitive amplifier. Because of noise generated in the switching circuit, this technique can only be used for beams with currents greater than 6 μA. This was found to be the minimum current detectable using cylindrical electrodes 6" in length and 3" in diameter. Ultimately changes will be made to improve this performance.

5.3 Secondary Emission Chambers

Several monitors based on the principle of secondary electron emission have been used to measure the position and profile of accelerator beams. A simple configuration of split electrodes such as that shown in Fig. 5.2 can be used to determine the beam position. Prudnikov et al. (1971) report a position sensitivity of ± 0.1 mm using just such a design. They used 35 μm thick Al foils, 40 mm in diameter and 5 mm apart. The emitting electrodes were cut in two equal halves and separated by 0.1 mm. A direct voltage of 300 V was applied to the collection electrodes. This type of monitor can also be used to measure beam profiles if provision is made to move each set of emitting electrodes across the beam in a direction perpendicular to the cut separating them. However, for profile measurements it is more common to use either a grid of foils or a single foil scanner. The SEM grid profile monitor consists of a series of horizontal and vertical foils mounted individually on two frames. Each foil is connected to its own amplifier or via a switch to a single amplifier. The resolution is determined by the distance between the foils, although it can be improved by one or more interpolation measurements. These are made by moving the slit assembly across the beam a distance equal to some fraction of the distance between the foils. This type of monitor has been used by Neet (1969) who reports a spatial resolution of 2.5 mm. He uses 2 mm wide Al foils spaced 5 mm apart. The secondary electrons

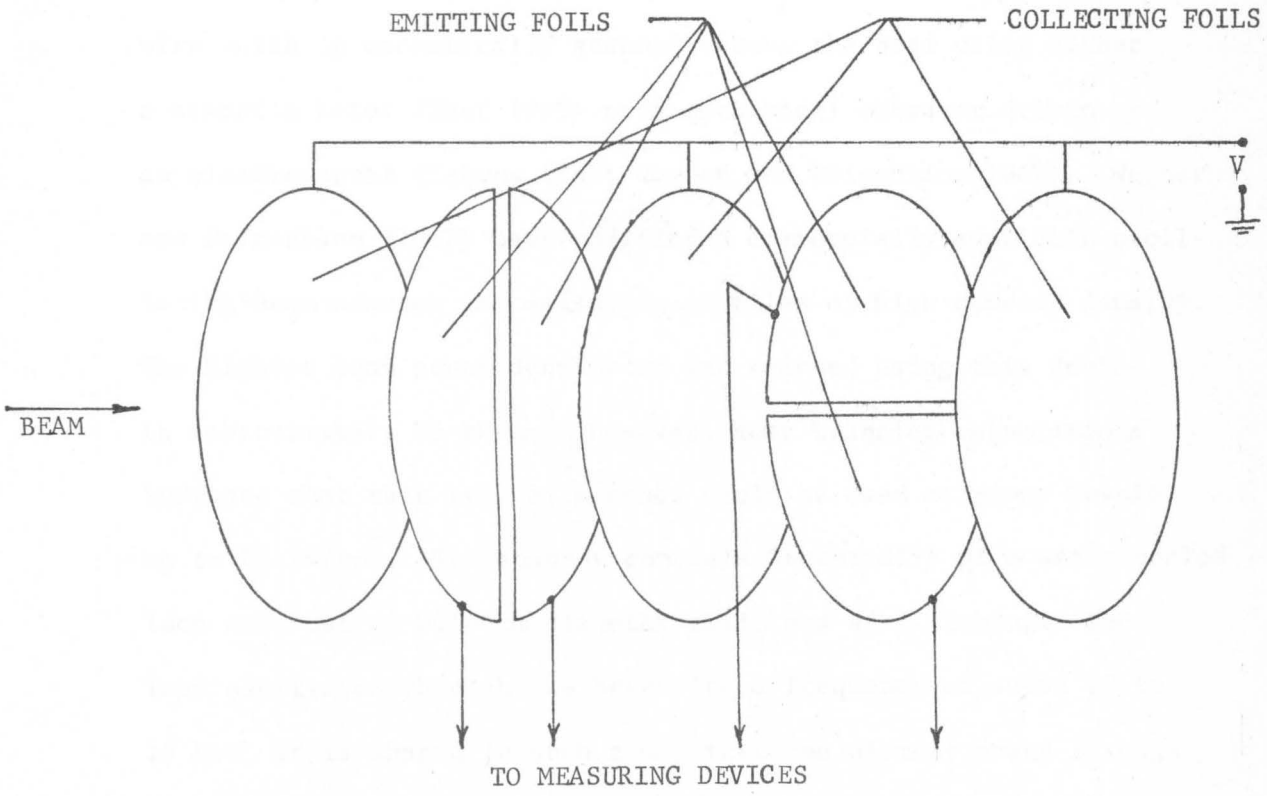

Fig. 5.2 A secondary emission beam position monitor

produced in these foils are trapped by three positive collector electrodes, the outer two of which are ring shaped so as not to intercept the beam. The average amount of material placed in the beam by this set of electrodes is 5.7 mg/cm^2.

The SEM profile scanner consists of a single foil or wire which is mechanically scanned across the beam using either a stepping motor (Neet 1969) or a mechanical vibrator driven by an electromagnet (Takacs 1965; Wegner and Feigenbaum 1967). Wegner and Feigenbaum (1967) have modified a commercially available oscillating beam scanner for measuring profiles of high current density. The highest beam power density so far scanned using this device is approximately 35 kW/cm^2; however, heat transfer calculations indicate that this type of scanner could be used at power levels up to 80 kW/cm^2. The scanner consists essentially of a water-cooled loop made out of 0.64 mm diameter stainless steel tubing. The loop oscillates through the beam with a frequency of about 10 to 15 Hz. It is shaped in such a way that one element scans through the beam in the x direction while another scans in the y direction. A combination of light source and photocell is used to mark the centre of the beam pipe in both the x and y directions. The spatial resolution of this device was observed to be 0.5 mm. The monitors used by Takacs (1965) and Neet (1969) are similar in design although no water cooling is provided. The design of these wire scanners reduces the amount of electronics required

and keeps the quantity of material placed in the beam to a minimum.

Thin foils mounted on motor-driven jaws can also be used to scan the beam. Each set of jaws would consist of one vertical and one horizontal pair of thin foils. The relative beam current can be determined by measuring the secondary electron current from the foils. By moving the jaws into the beam and recording the distance from the centre of the beam pipe when a certain integrated collected current is reached, a measure of the beam size can be obtained.

5.4 Residual Gas Ionization Beam Scanners

Because of the problem of beam degradation several beam position and profile monitors based on the ionization of the residual gas in the beam line vacuum system have been designed. Hornstra and de Luca (1967) have used devices of this type for beam observation in the Zero Gradient Synchrotron at ANL. They used an electric field to collect and accelerate the electrons resulting from the ionization of the gas in the beam line onto a phosphor screen or onto a set of strip electrodes. Beam widths at ANL are of the order of several centimeters and as a result no great demands were made on the spatial resolutions of these devices. The narrow beam widths at TRIUMF require better resolution than can be provided by these monitors. Johnson and Thorndahl (1968a) suggest that a strip electrode system, combined with a focussing magnetic

field along the direction of the electric field, could be used to provide a device having a spatial resolution of 1 to 2 mm. In order to cover the large beam apertures encountered at TRIUMF, a large number of electrode strips would be required and a suitable multiplexer system would have to be developed to process the signals from these electrodes. This problem can be avoided by collecting the electrons from the gas using some form of scanning system. Several such systems have been developed by Johnson and Thorndahl (1968 a.b.; 1969), the most successful of which is the crossed-field scanner shown schematically in Fig. 5.3. In this monitor crossed electric and magnetic fields are used to guide the electrons along the electric equipotential planes. The spatial distribution of the electron current travelling out along these equipotentials gives an orthogonal projection of the proton beam density distribution.

The electrons drift along the equipotentials with a velocity

$$v = E/B \tag{5.4.1}$$

following cycloid trajectories of radius

$$R = \frac{\left[\dot{z}_o^{\,2} + (\dot{y}_o - E/B)^2\right]^{\frac{1}{2}}}{eB/m} \tag{5.4.2}$$

where $\dot{z}_o$ and $\dot{y}_o$ are the initial electron velocity components along the direction of the magnetic field, B, and mutually perpendicular

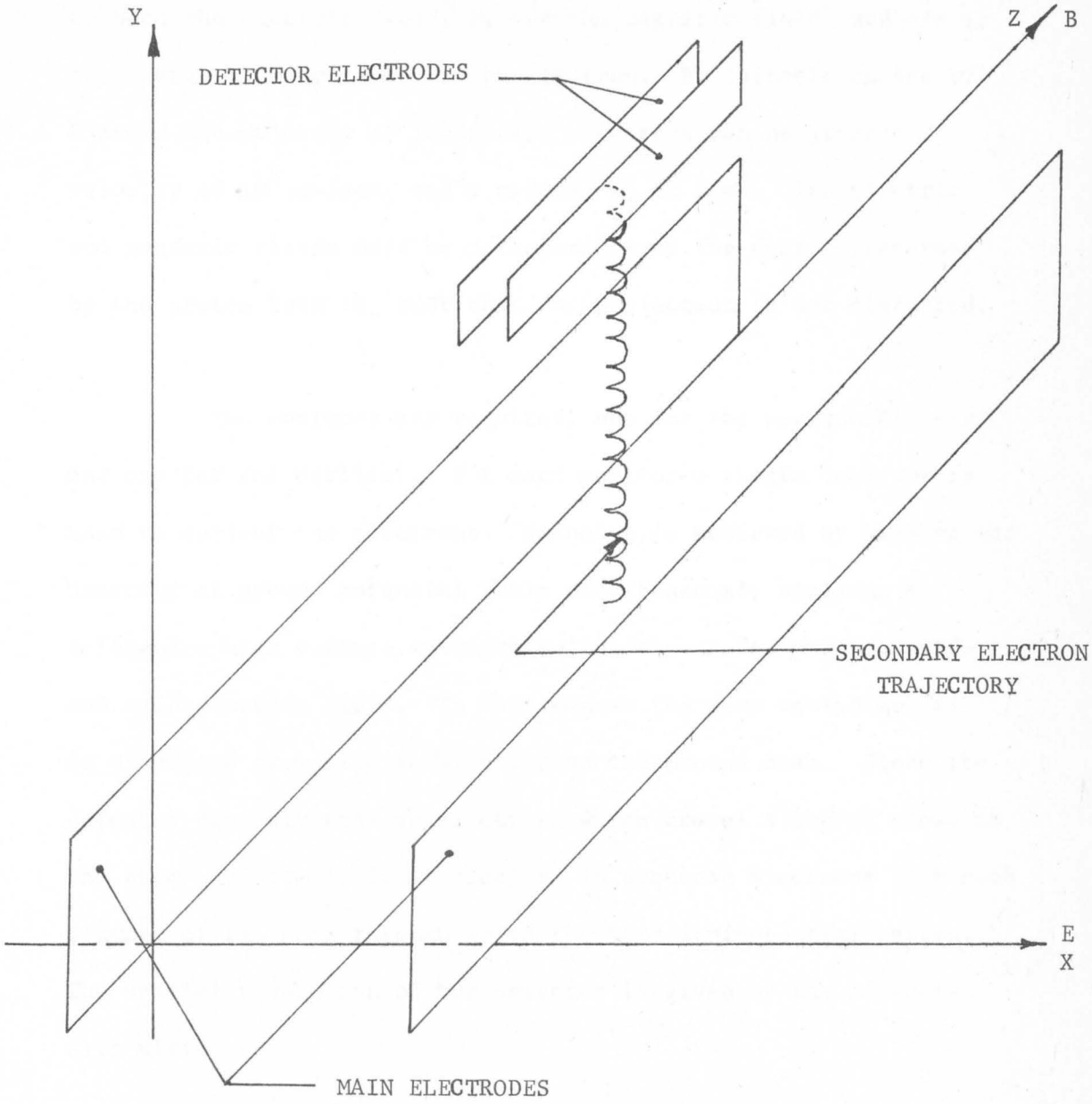

Fig. 5.3 The basic principle of the crossed-field scanner

to both the electric field, E, and the magnetic field, and e/m is the charge to mass ratio of the electron. By suitable choice of E and B the majority of ionization electrons can be given a velocity of 10^8 cm/sec and a radius, R, of 2 mm. The electric and magnetic fields must be orthogonal over the region traversed by the proton beam in order that the projection is not distorted.

Two monitors are required, one for the horizontal plane and one for the vertical. For each monitor a single detector is used to collect the electrons. Scanning is achieved by keeping the detector at ground potential while simultaneously applying a triangular high voltage waveform to the electrodes which provide the main electric field. In this manner the zero equipotential is displaced from side to side across the proton beam. Since the detector can only receive electrons which travel along or close to the zero equipotential, it receives in sequence electrons from each segment of the beam through which the zero equipotential passes. The spatial resolution of the detector is given by the effective slit width

$$s = \frac{a\ V_d}{V_e} \qquad (5.4.3)$$

where a is the separation of the main electrodes, V_e is the voltage between the main electrodes and V_d is the voltage between the detector electrodes. A resolution of 1 mm can be achieved with a field voltage of 300 volts/cm and a detector voltage of 30 volts.

The integrated output voltage produced at the detector is given by

$$v = \frac{p l t i_b}{C} \left(\frac{i_s}{i_b} \right) \qquad (5.4.4)$$

where i_s/i_b is the ratio of the electron ionization current, i_s, to the proton beam current, i_b, p is the residual gas pressure, l is the length of the detector along the beam direction, t is the scantime, and C is the detector capacity. From equation 4.4.2, i_s/i_b is 0.11/cm Torr for 500 MeV protons in air. Because of the large peak currents produced at the proton synchrotron accelerator at CERN ($i_b \sim 80$ mA), Johnson and Thorndahl were able to use scan-times of the order of 10 μsec and to operate at pressures of approximately 10^{-6} Torr. For t = 10 μsec, p = 10^{-6} Torr, l = 10 cm and C = 10 pf an output voltage of 80 mV was observed, compared to a background noise level of about 5 mV. Because of the smaller beam currents at TRIUMF longer scan-times will have to be used. For example, in the region downstream of Target T1 where the pressure is expected to be about 10^{-3} Torr, a scan-time of approximately 1 msec will be required to yield an output of 100 mV for a 1 μA proton beam assuming l = 10 cm and C = 10 pf. The noise level is expected to be the same as at CERN. In order to measure smaller intensities or the same intensity in a region of lower pressure still longer scan-times will be required. The possibility of introducing controlled leaks into the beam lines also exists.

5.5 Phosphor Screens, Scintillators and Čerenkov Counters

Phosphor screens and Cerenkov light monitors are widely used in accelerator facilities to monitor beam profiles (Bovet et al. 1964; Fabjan 1964; de Raad 1964). The screen monitors, which are a type of scintillator, have the advantage that they are easy to fabricate and show reasonably good sensitivity ($\sim$ 1 nA/cm^2 for ZnS). On the other hand their lifetime is severely limited by loss of luminescence as a result of exposure to the beam. Čerenkov counters show very good longevity but are substantially more expensive. Both types of monitors share a severe shortcoming that restricts their use to applications where rough, qualitative measurements are adequate. They suffer from saturation, a problem which is further accentuated by the vidicon of the TV camera used to monitor these devices.

More accurate profile measurements have been made using specially designed plastic scintillators. Kneissl and Kuhl (1970) use a thin rotating plastic scintillator viewed by a photomultiplier to measure beam position and profile. Peak currents down to 1 nA have been monitored using this device (shown in Fig. 5.4) and a spatial resolution of 1 mm has been achieved. Still more complex arrangements have been used by Binnie et al. (1964) and by Waters et al. (1962). These devices are again plagued by the problem of saturation at high beam intensities.

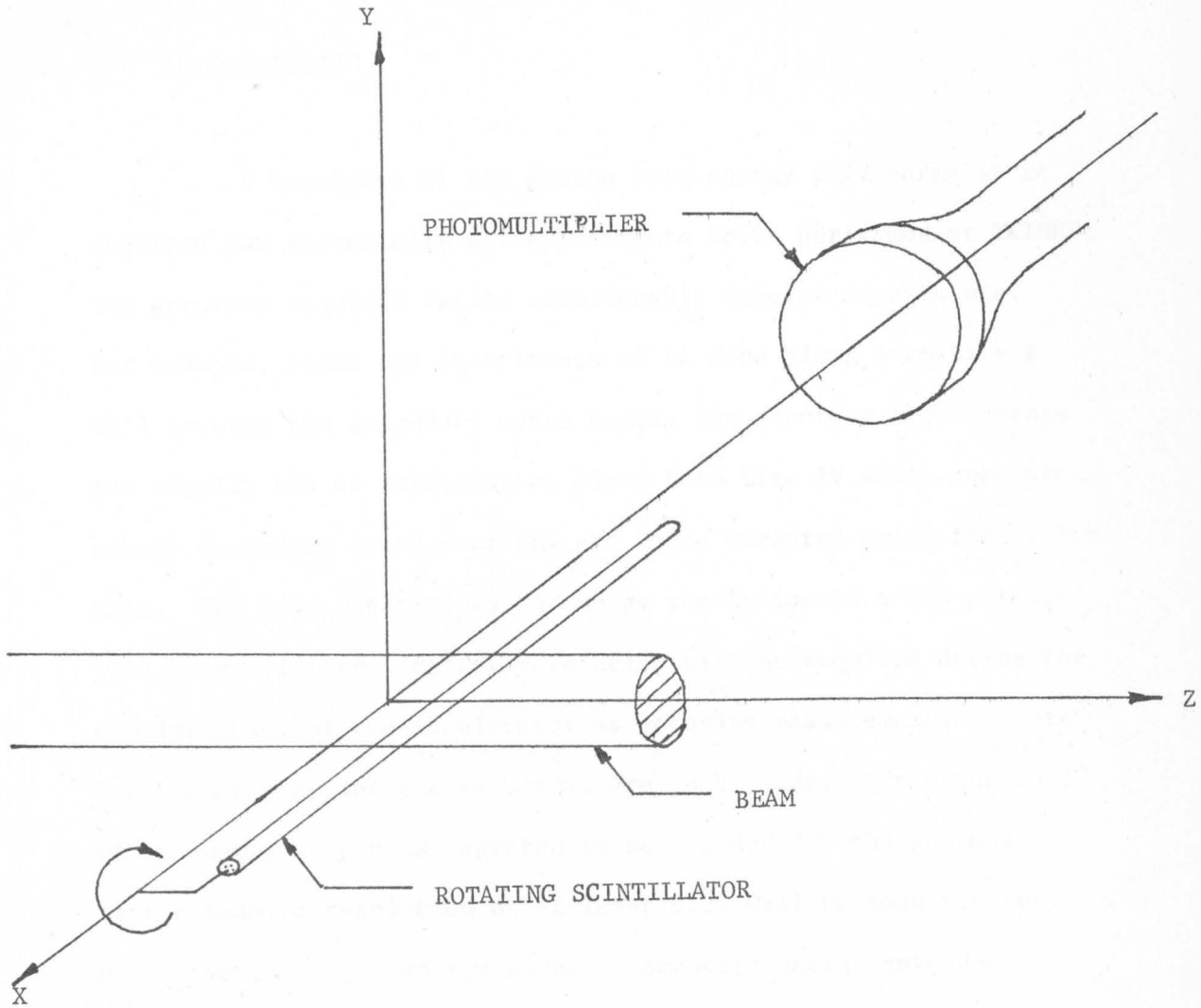

Fig. 5.4 A rotating scintillator profile monitor

CHAPTER 6

BEAM ENERGY MONITORS

6.1 Introduction

A knowledge of the proton beam energy will normally be required for essentially all experiments to be performed at TRIUMF; the accuracy required varies considerably amongst experiments. For example, since the experiments to be done along Beam Line I will involve the secondary meson beams, the accuracy requirements are usually not as stringent as along Beam Line IV where accurate energy dependent cross-sections are to be measured using the proton beam. For most experiments an energy resolution of a few percent will be sufficient. Better resolution will be required during the commissioning of the accelerator as accurate measurements of both the beam energy and energy spread are to be made. Since the full width energy spread is expected to be 1.2 MeV for the 500 MeV proton beam, a resolution of at least 0.2% will be required for measurements of the energy spread. Accurate energy spread measurements of the high resolution beams (ΔE = 50 keV) will require a resolution of 0.01%.

Beam energy measurements may be made using several techniques including: momentum analysis using a magnetic spectrometer, range-energy measurements, time-of-flight, Čerenkov counters, as well as several methods based on reaction kinematics (Smythe 1964). A

magnetic spectrometer mounted on Beam Line IV will provide the necessary accuracy to measure the energy and energy spread of TRIUMF's proton beams. However, for energy measurements on Beam Line I other methods must be made available.

6.2 Range-Energy Measurements

Range-energy measurements have been used extensively to determine the energy of medium energy particle beams (Chamberlain et al. 1957; Fretter 1961; Hanna and Hodges 1965; Stevens et al. 1971). The technique consists of measuring the range of particles in various materials for which the range-energy relationships are known. One of the major limitations of this method is that the best range-energy calculations (Barkas and Berger 1964) are only good to approximately 1%, and no adequate checks have been made to the data at higher energies. In addition, Landau broadening and range straggling cause problems in determining the range and as a result mask energy spreads of a few percent.

The two techniques most commonly used to measure the range of a particle are the range-energy telescope and the total energy scintillation counter. A telescope used by Stevens et al. (1971) to measure the range of 1025 MeV/c deuterons is shown in Fig. 6.1. It consists of four scintillation counters, numbered S_1 through S_4, and a variable aluminum degrader. The deuteron range

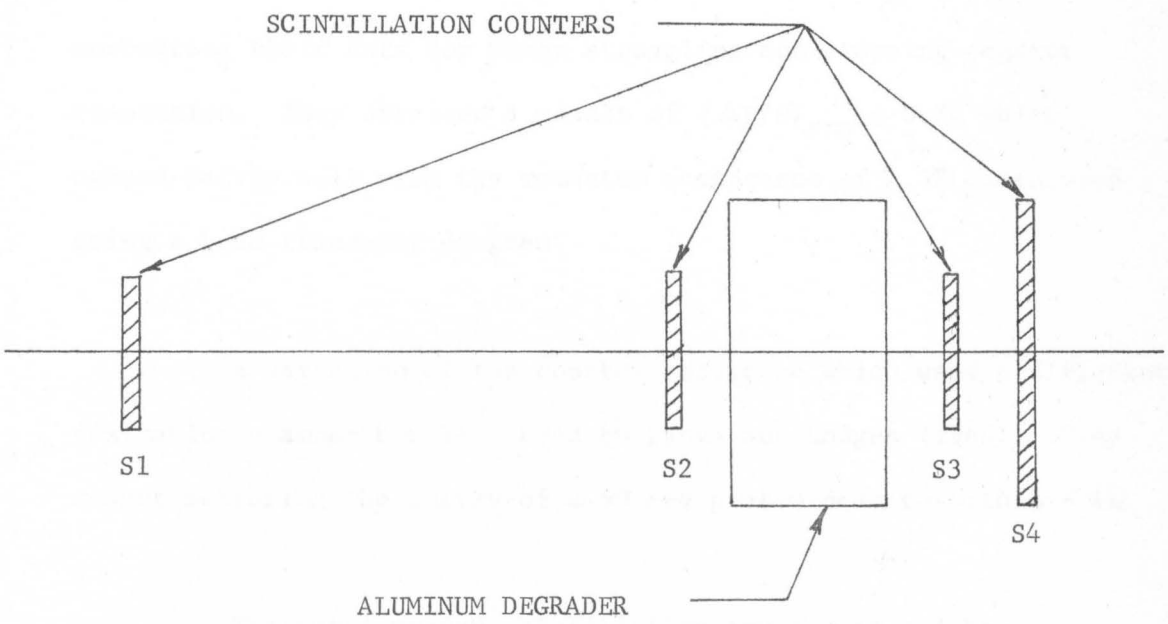

Fig. 6.1 A scintillation counter range-energy telescope

was measured by varying the amount of aluminum between S_2 and S_3. Differential range data were defined by the ratio of the coincidence $S_1S_2S_3\bar{S}_4$ to the monitor coincidence S_1S_2 with the S_1S_2 coincidence set to accept a narrow time region, including the deuteron peak, using time-of-flight techniques. Using this data Stevens et al. were able to determine the beam momentum to within ± 2.2 MeV/c. They were also able to estimate the beam momentum spread by correcting their data for range straggling and stopping counter resolution. They obtained a result of $(\Delta P/P)_{rms} = 0.7\%$ which agreed fairly well with the momentum acceptance of 0.5% calculated using a beam transport program.

A variation of the counter telescope which used a differential ionization chamber has been used by Hanna and Hodges (1965). They report measuring the energy of a 50 MeV proton beam to within ± 1%.

The total energy scintillation counter is a large scintillator in which the particle beam is stopped and the energy deposited is measured. In addition to range straggling, inelastic interactions in the total energy scintillator cause a tail in the light output for a monoenergetic proton beam; this tail makes it difficult to accurately determine the beam energy. One of the difficulties in using this device for monitoring high energy protons is its large size. A 500 MeV proton beam has a range of approximately 1 m in most scintillation materials. An excellent review of the

design of such large scintillators is given by Reynolds and Reines (1961).

Because the two techniques discussed use scintillation counters, they are limited to beams with intensities less than 10^7 particles/sec. They also require that large amounts of material ($\sim$ 100 gm/cm^2) be placed in the beam. As a result these techniques cannot be used to directly measure the energy of TRIUMF's proton beams except during beam alignment at very low intensities. At large intensities they could be used by measuring the energy of protons elastically scattered from a thin target placed in the primary beam. Location 3 seems ideal for this purpose.

6.3 Čerenkov Counters

The operation of a Čerenkov counter is based on the principle that when a charged particle passes through matter with a velocity, v, greater than the velocity of light in the material, u, electromagnetic radiation is emitted (Čerenkov 1937). The radiation is confined to a narrow conical shell around the direction of propagation of the particle. The angle of the aperature of this cone is given by (Jelley 1958)

$$\cos\theta = \frac{u}{v} = \frac{1}{n\beta} \qquad (6.3.1)$$

where n is the index of refraction of the material and $\beta = v/c$.

The intensity of Čerenkov radiation per unit pathlength per unit frequency interval is given by (Jelley 1958)

$$\frac{d^2N}{dxd\nu} = \frac{4\pi^2 e^2 z^2}{hc^2}\left[1 - \frac{1}{\beta^2 n^2(\nu)}\right] = \frac{2\pi z^2}{137c}\sin^2\theta \qquad (6.3.2)$$

where ν is the frequency of the emitted photons (Hz),

e is the electron charge,

z is the charge of the incident particle,

c is the velocity of light in vacuum (cm/sec), and

h is Planck's constant.

For a particle with z = 1 travelling in a medium of constant index of refraction, the number of photons in the visible spectrum generated per cm of pathlength is found by evaluating equation (6.3.2) to be

$$\frac{dN}{dx} \approx 500 \sin^2\theta \qquad (6.3.3)$$

For $\theta = 10^\circ$, this corresponds to approximately 15 photons/cm, compared with about 10^4 photons/cm produced by a minimum ionizing particle in plastic scintillator (Lindenbaum and Yuan 1961). However, this reduced current sensitivity should not be a problem at the beam intensities to be found at TRIUMF.

The Čerenkov counter operates by restricting the velocity range of the particles counted. This can be done in two ways. First of all Čerenkov radiation is only emitted for particles with velocities $\beta > 1/n$. Secondly, measurement of the angular range of the Čerenkov cone establishes that the incident particles have velocities in the

range $\beta_1 < \beta < \beta_2$, where β_1 and β_2 are determined by the index of refraction and the details of the measuring system. Several techniques for measuring this angular range are outlined in the article by Lindenbaum and Yuan (1961).

Having made the preceeding measurement, the energy of the incident beam can be found from

$$T = (\gamma - 1)\, M_o c^2 = \left[\frac{n \cos\theta}{\sqrt{n^2 \cos^2\theta - 1}} - 1 \right] M_o c^2 \qquad (6.3.2)$$

The energy resolution of the Čerenkov counter can be expressed in terms of the partial derivative

$$\frac{\partial\theta}{\partial T} = \frac{(1/\beta^2 - 1)^{3/2}}{M_o c^2 n \sin\theta} \qquad (6.3.5)$$

As shown in Table 6.1, counters designed for monitoring 200 to 500 MeV protons have a resolutions ranging from 0.1 to 0.5°/MeV. Since several authors have measured θ to within $\pm \frac{1}{2}°$ (Lindenbaum and Yuan 1961); these figures correspond to energy resolutions of the order of 0.5%. This agrees with the results of Mather (1951) who measured the energy of 340 MeV protons to within 0.3%, and with the calculations of Jelley (1958) who estimates that a resolution of 0.6 MeV should be obtainable for 275 to 800 MeV protons.

A measurement of the beam energy spread does not seem possible since several factors, in particular the divergence of the

T A B L E 6.1

The Characteristics of Cerenkov Counters Designed for Monitoring 200 and 500 MeV Proton Beams

Proton Beam Energy (MeV)	β	Index of Refraction n	θ	$\partial\theta/\partial T$ (°/MeV)
200	0.57	1.80	$11\frac{1}{2}^{\circ}$	0.52
500	0.76	1.35	13°	0.13

beam and optical dispersion caused by the fact that n is a function of the frequency of emitted photons, cause variations in θ which mask any effect due to energy spread. The dispersion width $\Delta\theta_D$ is expected to be about 0.5° to 1.0° depending on the radiator used, while the variation in θ caused by beam energy spread will only be 0.15° for the 500 MeV proton beam. A discussion of some of the other factors which can cause a broadening of the angular cone is given by Lindenbaum and Yuan (1961).

In conclusion, it should be mentioned that one need not intercept the entire proton beam nor is it necessary to use thick counters (1 mm should be sufficient). Furthermore, since one is not limited to counting individual particles this technique can be used at larger intensities ($\sim 1\ \mu A$) than the range-energy technique.

6.4 Monitoring Using Time-of-Flight Techniques

Conventional time-of-flight techniques have been used for determining the velocity of particle beams for many years (Manley and Jakobson 1965; Yuan and Lindenbaum 1961; Bruckmann et al, 1969; Brady et al. 1970; Stevens et al. 1971; Romero et al. 1972). The time-of-flight technique is usually accomplished by placing two detectors, such as scintillation counters, in the particle beam spaced a distance d apart and measuring the time it takes a beam pulse to travel between them. The time can be measured in a number

of ways, such as the coincidence method, measurement of the pulse separation on an oscilloscope screen, or using a time-to-amplitude converter. Several factors, including the resolution time of the coincidence circuit or the time-to-amplitude converter, and the risetime and dispersion of the output pulses from the detectors and photomultiplier tubes, limit the accuracy with which this time can be measured. The best time resolution obtainable for the measurement of the velocities of individual particles is approximately 1 nsec. However, because of the large beam intensities at TRIUMF one cannot count individual particles. Under TRIUMF beam conditions the scintillation counters will be saturated and one is forced to measure the time by observing the leading edge of the proton beam profile produced in these counters. A resolution of 0.5 nsec should be obtainable using this technique.

The major limitation of the time-of-flight method for measuring the energy of high energy beams is the large path lengths that are required. The longest path lengths available at TRIUMF are about 30 m in length. Since the kinetic energy of a particle beam is given by $T = (\gamma - 1) M_o c^2$, then

$$\frac{dT}{T} = \frac{\gamma^3 \beta^2}{\beta - 1} \frac{d\beta}{\beta} = \frac{\gamma^3 \beta^2}{\beta - 1} \frac{dt}{t} \qquad (6.4.1)$$

Given a 30 m flight path and a time resolution of 0.5 nsec an energy resolution of about 1% can be obtained for 200 to 500 MeV protons, as shown in Table 6.2. As a result, beam energy spread

T A B L E 6.2

Energy Resolution Obtainable Using Time-of-Flight Techniques

T (MeV)	β	$\frac{\gamma^3 \beta^2}{\beta - 1}$	Flight Time t (nsec)	$\frac{dt}{t}$	$\frac{dT}{T}$
200	0.57	2.7	175	2.9×10^{-3}	7.7×10^{-3}
500	0.76	4.0	130	3.9×10^{-3}	1.5×10^{-2}

measurements cannot be made using time-of-flight. In order to make energy measurements all energy degraders and targets must be removed from that section of beam line between the two counters. In conclusion, this technique has the advantages that it gives better results, requires much less material to be placed in the beam, and can be used at much higher intensities than the range-energy method. It is also less complex than the Čerenkov counter technique.

6.5 Proton-Electron Elastic Scattering

The energy of electrons produced at a known angle by elastic proton-electron scattering is directly related to the energy of the incident protons. For electrons scattered at 0° in the laboratory, $T_e = 2\ \beta^2 \gamma^2\ m_e$ where β and γ refer to the incident protons, and T_e and m_e are the energy and rest mass of the scattered electrons. For 500 MeV protons, T_e = 1.39 MeV. A proposal has been made by Gram (1971) to measure the energy of such electrons using lithium drifted germanium detectors and thereby determine the proton energy. He states that an energy resolution of 0.1% should be attainable for 500 MeV protons.

The kinematics of this process show that the best resolution can be obtained if one detects the electrons scattered at 0° since both the elastic scattering cross-section and the change in electron energy with proton energy, dT_e/dT_p, are largest

at 0° being 10^{-25} cm^2/sr and 2.5 keV/MeV, respectively, for 500 MeV protons. In addition $dT_e/d\theta = 0$ at $\theta = 0^{\circ}$. To measure the energy of 500 MeV protons to within 0.5 MeV, the electron energy must be measured to within 1.25 keV. This seems reasonable since the electron energy distribution for a monoenergetic 500 MeV proton beam has been calculated to be 13 keV wide; this width being due to spread in electron energy caused by the motion of these electrons in their atomic orbits. The detectors themselves have a full-width half-maximum resolution of 1 to 2 keV. One requirement of the technique is that one record sufficient events to be able to measure the centroid of the electron energy distribution to 10% of its full width at half maximum. 100 events should provide this accuracy. Since Gram (1971) has estimated that a 1 mg/cm^2 Be target yields 4×10^5 events/sec into 10^{-4} steradians at a proton beam intensity of 100 μA, the count rates are adequate at least down to intensities of the order of 1 nA (240 events/minute).

Although the proton energy can be measured to 0.1%, the energy spread cannot be measured since a 1.2 MeV wide proton beam produces a spread of only 3 keV in the electron energy distribution. However, apart from the magnetic spectrometer, this method appears to be the most accurate. It has the advantages that it can be simply calibrated using a radioactive electron source, and that it can be used throughout the operation of the TRIUMF accelerator if the foil is located at a point downstream of target T1 where the

beam degradation produced is not significant. The apparatus used in this technique should include a small permanent magnet to bend the scattered electrons out of the proton beam and focus them on a detector shielded from background radiation. Finally, it should be mentioned that this technique has applications as an absolute intensity monitor and as a device for measuring the muon contamination in pion beams (Gram 1971).

CHAPTER 7

SUMMARY AND CONCLUSIONS

The basic characteristics of the more important monitors discussed in this thesis are summarized in Tables 7.1, 7.2 and 7.3. From Table 7.1, it is seen that only the secondary emission monitor is capable of operating over the full range of proton beam intensities to be produced at TRIUMF. Such devices as the induction monitors and electrostatic probes are limited to operating at intensities greater than 1 μA and are less accurate than a secondary emission monitor (SEM). They also have a smaller signal-to-noise ratio and are severely restricted by the electrical environment. On the other hand, a SEM is an intercepting device and it also requires a reasonable vacuum in order to operate properly.

One of the most accurate intensity monitors is the ionization chamber. The large signal amplification of this device permits it to be used at low beam intensities. However, unlike the SEM saturation does occur when an ionization chamber is used to measure large beam currents.

One of the best absolute beam intensity monitors is the Faraday cup. It has the disadvantages of large size and high cost, and is limited to moderate currents because of power dissipation

T A B L E 7.1

Characteristics of the Major Intensity Monitors Discussed

Type	Range of Operation	Time Resolution	Accuracy	Remarks
Faraday cup	10 pA → 5 μA	~ 1 msec	2-3%	Best absolute monitor over this intensity range.
Induction monitors	usually > 1 μA	depends on circuit configuration	10%	Currents down to 30 nA can be measured at some expense. Response of device is independent of beam energy. nonintercepting
Electrostatic monitors	> 1 μA	depends on dircuit configuration	10%	Large surface area of electrodes poses pickup problems. nonintercepting
Ionization chambers (air filled, parallel plate)	> 10^5 p/sec	100 μsec	< 1%	Large signal amplification allows measurement of small beam intensities. Monitor saturates at large current densities (~ 1 mA/cm^2).
Secondary emission monitors	10 pA → 1 mA	~ 1 msec	~ 1%	No saturation occurs at least for current densities less than 150 mA/cm^2.
Activation techniques	limited by counters used to measure activation	------	5-10%	Accuracy depends on accuracy of cross-section measurements

TABLE 7.2

Characteristics of the Position and Profile Monitors Discussed

Type	Range of Operation	Parameter Measured	Resolution	Remarks
Electromagnetic pickup coils	> 10 nA	position	± 0.1 mm	Figures given are for tuned circuit design. nonintercepting
Electrostatic pickup electrodes	> 1 μA	position	± 0.1 mm	Uses resonant RF bridge tuned to cyclotron frequency. nonintercepting
Secondary emission monitors				
a) split electrodes		position	± 0.1 mm	Can be fastened to motor driven jaws and used to find beam size.
b) grid profile monitor	> 10 pA hitting any electrode	profile	2.5 mm	Resolution determined by distance between foils.
c) wire scanner		profile	0.5 mm	This type keeps material in beam to a minimum.
Residual gas ionization beam scanner	> 1 μA for $p = 10^{-3}$ Torr and t = 1 msec	profile	1.0 mm	Lower intensities can be measured using longer scan times, t, or at higher pressures.

T A B L E 7.3

Characteristics of the Beam Energy Monitors Discussed

Type	Range of Operation	*Energy Resolution	Remarks
Proton magnetic spectrometer	$< 10^5$ p/sec	< 0.03%	Spectrometer to be located in Proton Area. At present it is only method which can be used to measure beam energy spread as well as beam energy.
Range-energy measurements	$< 10^7$ p/sec	2-3%	Best range-energy calculations are good to only $\pm$1%.
Cerenkov counters	< 1 μA	0.5%	Can be used at larger currents if located to intercept only part of beam.
Time-of-flight	$< 10^7$/sec for individual particle counting	1%	Much larger currents can be tolerated if time between beam pulses is used to determine energy.
Proton-electron elastic scattering	> 1 nA	0.1%	Ideal for use at large currents.

*Figures are for 500 MeV protons

problems. It is recommended that a Faraday cup be incorporated with one of the beam dumps in the proton area.

The activation technique as well as the techniques discussed in Section 4.7 cannot be used to monitor TRIUMF's proton beams during normal beam operation. However they can be used during beam set up and alignment and in the experimental areas where very low intensities are found. Since the activation technique will probably be the most generally used absolute beam intensity monitor, it is recommended that as part of the experimental program more accurate determinations of activation cross-sections be made by using the Faraday cup or single particle counting of the beam at low intensity.

The best position and profile monitor again appears to be some form of a secondary emission device. The SEM wire scanner has a resolution of 0.5 mm and can be used in those locations where one wishes to keep the amount of material in the beam to a minimum. Residual gas ionization beam scanners prove useful when the optics of the beam transport system requires that no material be placed in the beam. The resolution obtainable is comparable to that of the SEM. However one is limited to operating at larger currents. Electromagnetic and electrostatic pickup are nonintercepting devices as well, but can only be used for measuring beam position and not beam profile. Čerenkov counters, phosphor screens and other scintillators can be put to good use during beam alignment where rough

measurements of the position and profile are adequate.

The best energy monitor is the proton spectrometer which is to be built and located in the proton area. It is at present the only device accurate enough to measure the energy spread of the proton beams anticipated. Proton-electron elastic scattering and time-of-flight can be used to measure the beam energy at large intensities, but the latter will require removing the meson production targets on Beam Line I during the measurements. Range-energy measurements must be done at low intensities and are the least accurate. They also require large amounts of material to be placed in the beam. Cerenkov counters can be used at larger intensities and are more accurate than range-energy measurements.

Much work remains to be done in order that the most suitable monitors are provided to both the machine operator and the experimenter. More detailed studies must be done on the effect of placing intercepting beam monitors at the various locations desired. Such factors as cost and availability of commercially available devices have not been considered in this work.

In conclusion this thesis provides a basic review of the various monitors which have been used on existing accelerators and which are best suited to monitor the external proton beams produced at TRIUMF.

REFERENCES

Aggson, T.L. 1962. The secondary emission monitor. Linear Accelerator Laboratory Report L.A.L. 1028, Orsay, France.

Agoritsas, V. 1968. Secondary emission chambers for monitoring the CPS ejected beams. In Symposium on Beam Intensity Measurement, edited by V.W. Hatton and S.A. Lowndes, pp 117-151, Daresbury Nuclear Physics Laboratory, England.

Allison, R.W., Evans, D.M., Richter, R.M., Sherwood, A.J., and Zajec, E. 1966. Measurements of the linear accelerator exit beam of the bevatron injector. Lawrence Radiation Laboratory Report UCRL-17001.

Auld, E. 1971. Private communication.

Banford, A.P. 1966. The Transport of Charged Particle Beams. E. and F.N. Spon Ltd., London.

Barkas, W. and Berger, M. 1964. Tables of energy losses and ranges of heavy charged particles. NASA Report SP-3013.

Battisti, S. 1966. Fast ejected beam monitor. CERN Internal Report MPS/Int. CO 66-1.

Beer, G.A. and Smith, D.F. 1971. Conceptual design of Beam Line I vacuum system. TRIUMF Internal Report VPN-71-28.

Bergère, R., Delezenne, E., and Veyssière, A. 1962a. A study of current monitors for an electron linear accelerator. Nucl. Instr. Meth. 15, 327.

Bergère, R., Veyssière, A., and Daujat, P. 1962b. Linac beam position monitor. Rev. Sci. Instr. 33, 1441.

Bergstrom, J.C. 1963. Linac beam current and beam position sensors. University of Saskatchewan Internal Report 10.

Bertini, H.W. 1963. Low energy intranuclear cascade calculation. Phys. Rev. 131, 1801.

Bertini, H.W. 1965. Erratum: Low energy intranuclear cascade calculation. Phys. Rev. 138, AB2.

Binnie, D.M., Duane, A., Miller, D.B., Neale, W.W., Newth, J.A., Potter, D.C., and Walters, J.A. 1964. Visual observation of beam profiles. Nucl. Instr. Meth. 31, 153.

Blankenburg, S.A., Cobb, J.K., and Muray, J.J. 1965. Efficiency of secondary electron emission monitors for 70 MeV electrons. SLAC Report SLAC-PUB-107.

Bogaards, J.J.W. and Drake, T.E. 1966. A non-intercepting beam position, beam current and pulse shape monitor for pulsed accelerators. Nucl. Instr. Meth. 42, 297.

Bovet, C. 1964. Measurements on slow beam-ejection from the CERN PS. CERN Report 64-25.

Brady, F.P., Knox, W.J., and Johnson, S.W. 1970. Energy measurements of the 20-60 MeV neutron beam of the Davis 76 inch isochronous cyclotron. Nucl. Instr. Meth. 89, 309.

Brown, K.L. and Tautfest, G.W. 1956. Faraday cup monitors for high energy electron beams. Rev. Sci. Instr. 27, 696.

Bruckmann, H., Haase, E.L., Kluge, E., and Schanzler, L. 1969. A novel time-of-flight method and its applications in nuclear reaction studies. Nucl. Instr. Meth. 67, 29.

Caldwell, D.O. 1961. Monitoring high energy proton beams. In Techniques of High Energy Physics, edited by D.M. Ritson, pp 487-507, Interscience Publishers Inc., New York.

Čerenkov, P.A. 1937. Visible radiation produced by electrons moving in a medium with velocities exceeding that of light. Phys. Rev. 52, 378.

Chamberlain, O., Segrè, E., Tripp, R.D., Wiegand, C., and Ypsilantis, T. 1957. Experiments with 315 MeV polarized protons: proton-proton and proton-neutron scattering. Phys. Rev. 105, 288.

Chan, C., Hunt, D.W., and Lobb, D.E. 1972. TRANS-a program to design beam transport systems. TRIUMF Internal Report TRI-I-72-2.

Cumming, J.B. 1963. Monitor reactions for high energy proton beams. Ann. Rev. Nucl. Sci. 13, 261.

de Parry, T. and Ratner, L.G. 1969. Evaluation of high stability secondary emission monitors. IEEE Trans. Nucl. Sci. NS-16, 923.

de Raad, B. 1963. The application of synchrotron light for beam observation in the BSY. SLAC Technical Note SLAC-TN-63-95.

de Raad, B. 1964. Beam profile monitors for the beam switchyard. SLAC Technical Note SLAC-TN-64-77.

Dorikens-Vanpraet, L., Van Camp, K., Dorikens, M., and Callebaut, D. 1967. An improved non-intercepting accelerator beam position sensor. Nucl. Instr. Meth. 47, 58.

Duelli, B. 1969. The internal beam probes. TRIUMF Design Note TRI-DN-69-29.

Duelli, B. 1971. Private communication.

Fabjan, C.W. and Zulliger, H. 1964. Survey of beam monitor possibilities for the ejected beam at the CPS east area. CERN Internal Report MPS/DL/Int. 64-21.

Fabjan, C.W. 1964. Use of scintillating fibres and standard T.V. equipment for monitoring of external proton beams at the CPS. CERN Internal Report MPS/DL/Int. 64-23.

Fretter, W.B. 1961. Measurements of range and energy with cloud chambers and bubble chambers. In Methods of Experimental Physics, edited by C.L. Yuan and C.S. Wu, 5A, pp 436-437, Academic Press, New York.

Fulbright, H.W. 1958. Ionization chambers. In Handbuch der Physik, edited by S. Flugge, 45, pp 1-51, Springer-Verlag, Berlin.

Glavina, C. 1971. Private communication.

Gram, P.A.M. 1971. Beam energy and intensity measurements by p-e scattering. In Proc. LAMPF Summer Study Session, edited by R.J. Macek, E.R. Martin, J.E. Simmons and K.E. Harper, pp 43-44, Los Alamos Scientific Laboratory, New Mexico.

Greening, J.R. 1954. A survey of surface back-scatter factors for radiation generated at 200 to 250 kV. Brit. J. Radial. 27, 532.

Grossetête, B. and Isabelle, D.B. 1968. Beam monitoring at Orsay. In Symposium on Beam Intensity Measurement, edited by V.W. Hatton and S.A. Lowndes, pp 3-19, Daresbury Nuclear Physics Laboratory, England.

Hanna, R.C. and Hodges, T.A. 1965. A differential ion chamber for beam energy measurement. Nucl. Instr. Meth. 37, 346.

Hatton, V.W. 1968. The Daresbury Faraday cup. In Symposium on Beam Intensity Measurement, edited by V.W. Hatton and S.A. Lowndes, pp 99-104, Daresbury Nuclear Physics Laboratory, England.

Hatton, V.W. and Lowndes, S.A. (editors) 1968. Symposium on Beam Intensity Measurement. Daresbury Nuclear Physics Laboratory, England.

Harting, D., Kluyver, J.C., and Kusumegi, A. 1960. Absolute intensity measurements on the external proton beam of the CERN synchro-cyclotron. CERN Report 60-17.

Hodges, T.A. 1971. Thin windows in intense proton beams. TRIUMF Internal Report VPN-71-23.

Hohbach, R. and Mango, S. 1967. An inductive beam monitor for the extracted proton beam of the CERN synchro-cyclotron. CERN Report 67-9.

Holcomb, L., Porat, D.L., and Robinson, K. 1963. Measuring position and current of an accelerated particle beam. Nucl. Instr. Meth. 24, 399.

Hornstra, F. and de Luca, W.H. 1967. Non-destructive beam profile detection systems for the Zero Gradient Synchrotron. Argonne National Laboratory Internal Report.

Isabelle, D.B. and Roy, P.H. 1963. Factors influencing the stability of a secondary emission monitor. Nucl. Instr. Meth. 20, 17.

James, P.W. 1971. Moliere scattering distributions for 500 MeV protons on 4 mg/cm^2, 4 gm/cm^2 and 20 gm/cm^2 carbon targets. TRIUMF Internal Report VPN-71-2.

James, P.W. 1972. To be published as a TRIUMF Internal Report.

Jelley, J.V. Cerenkov Radiation and its Applications. Permagon Press, New York.

Johnson, C.D. and Thorndahl, L. 1968a. Non-destructive proton beam profile scanners for the CPS, based on the ionization of residual gas in the beam vacuum chamber. CERN Internal Report MPS/Int. CO 68-8.

Johnson, C.D. and Thorndahl, L. 1968b. The CPS ionization beam scanner. CERN Internal Report MPS/Int. CO 68-13.

Johnson, C.D. and Thorndahl, L. 1969. The CPS gas-ionization beam scanner. IEEE Trans. Nucl. Sci. NS-16, 909.

Johnson, K., Klippert, T., and Ramler, W.J. 1961. A non-intercepting accelerator beam position sensor. Nucl. Instr. Meth. 14, 125.

Johnson, K. and Ramler, W.J. 1963. Cyclotron beam position sensor. CERN Report 63-19.

Kantz, A.D. and Hofstadter, R. 1952. Electron-induced showers in copper. Phys. Rev. 89, 3.

Kantz, A.D. and Hofstadter, R. 1954. Large scintillators, Cerenkov counters for high energies. Nucleonics 12, 36.

Karzmark, C.J. 1964. Secondary emission monitor as a linear accelerator beam dose monitor. Rev. Sci. Instr. 35, 1646.

Kneissl, U. and Kuhl, G. 1970. Ein empfindlicher profil-und positionsmonitor fur elektronen und positronenstrahlen. Nucl. Instr. Meth. 87, 77.

Lapostolle, P.M. and Septier, A.L. (editors) 1970. Linear Accelerators. North-Holland Publishing Co., Amsterdam.

Larsen, R.S. 1966. Design of beam position and charge monitoring circuits for the Stanford two-mile accelerator. SLAC Report No. 63.

Larsen, R.S. and Horelick, D. 1968. A precision toroidal charge monitor for SLAC. In Symposium on Beam Intensity Measurement, edited by V.W. Hatton and S.A. Lowndes, pp 260-279, Daresbury Nuclear Physics Laboratory, England.

Larsen, R.S. and Horelick, D. 1969. Digital computer error analysis of a resonant toroid charge monitor. SLAC Report No. 100.

Larsen, R.S. 1971. Toroidal charge monitoring systems. In Proc. LAMPF Summer Study Session, edited by R.J. Macek, E.R. Martin, J.E. Simmons and K.E. Harper, pp 25-30, Los Alamos Scientific Laboratory, New Mexico.

Law, L.A. and Holcomb, L. 1965. The Cambridge electron accelerator beam position monitors. IEEE Trans. Nucl. Sci. NS-12, 856.

Lindenbaum, S.J. and Yuan, C.L. 1961. Cerenkov counters. In Methods of Experimental Physics, edited by C.L. Yuan and C.S. Wu, 5A, pp 162-193, Academic Press, New York.

Lobb, D.E. 1971. Current status of the design of Beam Line I to Target T1. TRIUMF Internal Report VPN-71-18.

Macek, R.J., Martin, E.R., Simmons, J.E., and Harper, K.H. (editors) 1971. Symposium on Beam Intensity Measurement. Los Alamos Scientific Laboratory, New Mexico.

Mackenzie, G.H. 1969. Cyclotron stripping foils and targets. TRIUMF Design Note TRI-DN-69-15.

Mackenzie, G.H. and Craddock, M.K. 1970. Private communication.

Manley, J.H. and Jakobson, M.J. 1954. Cyclotron beam energy determination by a time-of-flight method. Rev. Sci. Instr. 25, 368.

Marquez, L. 1952. The yield of F^{18} from medium and heavy elements with 420 MeV protons. Phys. Rev. 86, 405.

Mather, R.L. 1951. Cerenkov radiation from protons and the measurement of proton velocity and kinetic energy. Phys. Rev. 84, 181.

Molière, G. 1948. Theory of the scattering of rapid charged particles. Atomic Energy Research Establishment Report Lib./Trans. 626, Harwell, England.

Nagel, H.H. 1965. Electron-photon cascades in lead, Monte Carlo calculations for primary electron energies between 100 and 1000 MeV. Z. Phys. 186, 319.

Neal, R.B. (editor) 1968. The Stanford Two-Mile Accelerator. W.A. Benjamin, Inc., New York.

Neet, D.A.G. 1969. Beam profile monitors for fast and slow extracted proton beams. IEEE Trans. Nucl. Sci. NS-16, 914.

Okabe, S., Tabata, T., and Ito, R. 1961. Nonobstructive low energy electron beam monitor. Rev. Sci. Instr. 32, 1347.

Olsen, D. 1965. Design of a precision current integrator for the BSY. SLAC Technical Note SLAC-TN-65-56.

Planskoy, B. 1963. Secondary electron emission from aluminum foils in high energy beam monitors. Nucl. Instr. Meth. 24, 172.

Prokoshkin, I.D. and Tiapkin, A.A. 1957. Investigation of the excitation functions for the reactions $C^{12}(p, pn)C^{11}$, $Al^{27}(p, 3pn)Na^{24}$, and $Al^{27}(p, 3p, 3n)Na^{22}$ in 150-660 MeV energy range. Soviet Physics JETP. 5, 148.

Prudnikov, I.A., Toropov, A.S., and Chichikalov, Y.F. 1972. Design and sensitivity of a secondary emission monitor of accelerated electron position. Nucl. Instr. Meth. 101, 275.

Ranft, J. 1967a. Improved Monte-Carlo calculation of the nucleon-meson cascade in shielding material: description of the method of calculation. Nucl. Instr. Meth. 48, 133.

Ranft, J. 1967b. Improved Monte-Carlo calculation of the nucleon-meson cascade in shielding material: comparison of the results for incident proton beams with momenta of 10 and 20 GeV/c with experimental data. Nucl. Instr. Meth. 48, 261.

Ranft, J. 1970. Monte-Carlo calculation of energy deposition by the nucleon-meson cascade and total-absorption-nuclear-cascade (TANC) counters. Nucl. Instr. Meth. 81, 29.

Reeve, P.A. 1971. Conceptual design of a "pre-quad" septum scattering pion channel. TRIUMF Internal Report VPN-71-22.

Reynolds, G.T. and Reines, F. 1961. Scintillation counters and luminescent chambers. In Methods of Experimental Physics, edited by C.L. Yuan and C.S. Wu, pp 120-161, Academic Press, New York.

Richardson, J.R. 1969. Energy resolution in a 500 MeV H^- cyclotron. TRIUMF Report TRI-69-6.

Richardson, J.R. and Craddock, M.K. 1969. Beam quality and expected energy resolution from the TRIUMF cyclotron. TRIUMF Preprint TRI-PP-69-8.

Ritson, R.M. (editor) 1961. Techniques of High Energy Physics. Interscience Publishers Inc., New York.

Romero, J.L., Massmann, H., Brady, F.P., and Zamudio, J. 1972. A simple time-of-flight method to measure the beam energy of a cyclotron. Nucl. Instr. Meth. 100, 551.

Rossi, B. and Griessen, K. 1941. Cosmic ray theory. Rev. Mod. Phys. 13, 240.

Sharp, J.B. 1962. The induction type beam monitor for the PS ("Hereward transformer"). CERN Internal Report MPS/Int. CO 62-15.

Shea, R.F. (editor) 1965. Proc. 1st National Particle Accelerator Conference. IEEE. Trans. Nucl. Sci. NS-12.

Shea, R.F. (editor) 1967. Proc. 1967 Particle Accelerator Conference. IEEE Trans. Nucl. Sci. NS-14.

Shea, R.F. (editor) 1969. Proc. 1969 Particle Accelerator Conference. IEEE Trans. Nucl. Sci. NS-16.

Shea, R.F. (editor) 1971. Proc. 1971 Particle Accelerator Conference. IEEE Trans. Nucl. Sci. NS-18.

Sherwood, A.J. 1965. Electrostatic induction electrode systems for beam position detection. IEEE Trans. Nucl. Sci. NS-12, 925.

Simanton, J.R. 1969. Calibrating induction electrodes using cathode ray beams. IEEE Trans. Nucl. Sci. NS-16, 932.

Smythe, R. 1964. Relativistic equations and tables for ion energy determination by the crossover technique. Rev. Sci. Instr. 35, 1197.

Steinberg, E.P. 1971. Intensity measurements by the activation method: proton and pion beams. In Proc. LAMPF Summer Study Session, edited by R.J. Macek, E.R. Martin, J.E. Simmons and K.E. Harper, pp 33-40, Los Alamos Scientific Laboratory, New Mexico.

Stevens, A.J., Schwartz, D.M., Rush, C.J., Reibel, K., Romanowski, R.L., Sumner, R.L., Swallow, E.C., Watson, J.M., Winston, R., and Wolfe, D.M. 1971. Direct momentum determination of a medium energy particle beam using time-of-flight and range techniques. Nucl. Instr. Meth. 97, 207.

Taimuty, S.I. and Deaver, B.S. 1961. Transmission current monitor for high energy electron beams. Rev. Sci. Instr. 32, 1098.

Takacs, J. 1965. Beam scanner for the Oxford electrostatic tandem accelerator. IEEE Trans. Nucl. Sci. NS-12, 980.

Tautfest, G.W. and Fechter, H.R. 1955. A nonsaturable high-energy beam monitor. Rev. Sci. Instr. 26, 229.

Taylor, L.S. 1951. The measurement of X and gamma radiation over a wide energy range. Brit. J. Radial. 24, 67.

Trump, M. 1971. A current monitoring system for H^- and polarized proton beams at LAMPF. In Proc. LAMPF Summer Study Session, edited by R.J. Macek, E.R. Martin, J.E. Simmons and K.E. Harper, pp 31-32, Los Alamos Scientific Laboratory, New Mexico.

Unser, K. 1969. Beam current transformer with D.C. to 200 MHz range. IEEE Trans. Nucl. Sci. NS-16, 934.

Vanhuyse, V.J. and Van de Vijver, R.E. 1962. Efficiency of secondary emission monitors for electron beams. Nucl. Instr. Meth. 15, 63.

Vanhuyse, V.J., Wattecamps, E.D., Van de Vijver, R.E. and Vanpraet, G.J. 1962. Secondary emission beam monitors for 0.5 to 3.5 MeV electrons. Nucl. Instr. Meth. 15, 59.

Völkel, U. 1965. DESY Report 65/6, German Accelerator Laboratory, Hamburg, Germany.

Waters, J.R., Reynolds, G.T., Scarl, D.B. and Zdanis, R.A. 1962. A scintillation chamber-image intensifier beam profile detector. Nucl. Instr. Meth. 17, 44

Wegner, H.E. and Feigenbaum, I.L. 1967. High current beam scanner. IEEE Trans. Nucl. Sci. NS-14, 1099.

Williard, H.B. and Riley, P. 1971. Preliminary design considerations for an 800 MeV proton beam Faraday cup. In Proc. LAMPF Summer Study Session, edited by R.J. Macek, E.R. Martin, J.E. Simmons and K.E. Harper, pp 41-42, Los Alamos Scientific Laboratory, New Mexico.

Wilson, C.W. 1954. Observations on the ionization produced by radium gamma rays in air-walled ionization chambers at low gas pressures. Brit. J. Radial. 27, 158.

Yamada, R. 1962. New magnetic pickup probe for charge particle beams. Japan. J. Appl. Phys. 1, 92.

Yount, D. 1967. A high precision Faraday cup and quantameter for SLAC. Nucl. Instr. Meth. 52, 1.

Yount, D. 1968. A high precision Faraday cup and quantameter for SLAC. In Sumposium on Beam Intensity Measurement, edited by V.W. Hatton and S.A. Lowndes, pp 75-96, Daresbury Nuclear Physics Laboratory, England.

Yuan, C.L. and Wu, C.S. (editors) 1961. Methods of Experimental Physics. 5A, Academic Press, New York.

Yuan, C.L. and Lindenbaum, S.J. 1961. Time-of-flight method. In Methods of Experimental Physics, edited by C.L. Yuan and C.S. Wu, 5A, pp 438-443, Academic Press, New York.

Zulliger, H. 1964. Investigations with the use of electromagnetic and electrostatic beam monitors in the slow ejected beam of the CPS. CERN Internal Report MPS/Int. DL 64-21.

Surname: JAMES Given Names: PETER WILLIAM

Place of Birth: PRINCE RUPERT, B.C. Date of Birth: APRIL 19, 1947

Educational Institutions Attended, with Dates of Entering and Leaving:

UNIVERSITY OF VICTORIA, VICTORIA 1965 to 1969

Degrees, Diplomas, Etc., Awarded, with Dates and Names of Institutions:

B.Sc. (Honours) 1969 University of Victoria, Victoria

Honours and Awards:

N.R.C. Scholarships, 1969/70, 1970/71 and 1971/72

THE UNIVERSITY OF VICTORIA LIBRARY

MANUSCRIPT THESIS

AUTHORITY TO DISTRIBUTE

AUTHOR: This thesis may be lent or microfilm copies made available:

(a) Without restriction

(b) With the restriction that, for a period of five years (until December 1977) the written approval of the following is required:

(1) The Chairman, School of Graduate Studies .....

(2) The Author .....

(3) both the Chairman, School of Graduate Studies, and the Author .....

BORROWERS: The borrower undertakes, by signing below, to give proper credit for any use made of the thesis, and to obtain the consent of the author if it is proposed to make extensive quotations, or to reproduce the thesis in whole or in part.

Signature of Borrower	Address	Date